Journal of Medicinal Chemistry

Article

Discovery of Novel Aminotetralines and Aminochromanes as Selective and Competitive Glycine Transporter 1 (GlyT1) Inhibitors

Willi Amberg, Udo E.W. Lange, Michael Ochse, Frauke Pohlki, Berthold Behl, Ana Lucia Relo, Wilfried Hornberger, Carolin Hoft, Mario Mezler, Jens Sydor, Ying Wang, Hongyu Zhao, Jason T. Brewer, Justin Dietrich, Huanqiu Li, Irini Akritopoulou-Zanze, Yanbin Lao, Steven M Hannick, Yi-Yin Ku, and Anil Vasudevan

J. Med. Chem., **Just Accepted Manuscript** • Publication Date (Web): 06 Aug 2018

ACS Publications

is published by the American Chemical Society. 1155 Sixteenth Street N.W., Washington, DC 20036

Discovery of Novel Aminotetralines and Aminochromanes as Selective and Competitive Glycine Transporter 1 (GlyT1) Inhibitors

Willi Amberg,[†] Udo E. W. Lange,[†] Michael Ochse,[†] Frauke Pohlki,[†] Berthold Behl,[†,⊥] Ana Lucia Relo,[†] Wilfried Hornberger,[†] Carolin Hoft,[†] Mario Mezler,[†] Jens Sydor,[‡] Ying Wang,[‡] Hongyu Zhao,[‡] Jason T. Brewer,[‡] Justin Dietrich,[‡] Huanqiu Li,[‡] Irini Akritopoulou-Zanze,[‡] Yanbin Lao,[‡,§,⊥] Steven M. Hannick,[‡] Yi-Yin Ku,[‡] Anil Vasudevan[‡]*

[†]AbbVie Deutschland GmbH & Co. KG, Neuroscience Research, Knollstrasse, 67061 Ludwigshafen, Germany

[‡]AbbVie Inc., 1 North Waukegan Rd., North Chicago, IL 60064, United States.

ABSTRACT: The glycine transporter 1 (GlyT1) has emerged as a key novel target for the treatment of schizophrenia. Herein, we report the synthesis and biological evaluation of aminotetralines and aminochromanes as novel classes of competitive GlyT1 inhibitors. Starting from a high-throughput screening hit, structure-activity relationship studies led first to the discovery of aminotetralines displaying high GlyT1 potency and selectivity, with favorable pharmacokinetic properties. Systematic investigations of various parameters (e.g. topological polar surface area, number of hydrogen bond donors) guided by *ex vivo* target occupancy evaluation, resulted in lead compounds possessing favorable brain penetration properties as **(7*S*,8*R*)-27a**. Further optimization revealed compounds with reduced efflux liabilities as aminochromane **51b**. In an *in vivo* efficacy model **(7*S*,8*R*)-27a** dose-dependently reversed

L-687,414 induced hyperlocomotion in mice with an ED_{50} of 0.8 mg/kg. All these results suggest **(7*S*,8*R*)-27a** and **51b** as a new GlyT1 inhibitors worthy of further profiling.

INTRODUCTION

Impaired N-methyl-D-aspartate receptor (NMDA receptor) mediated neurotransmission has been implicated in schizophrenia. A role of hypofunctional NMDA receptor signaling supported by clinical observations is that NMDA receptor antagonists can induce the whole spectrum of schizophrenia symptoms [1-5] and by the discovery of schizophrenia susceptibility genes which are involved in or interfere with NMDA receptor signaling.[6-8]

Neurophysiological findings on an imbalance between excitation and inhibition, on dysfunctional micro-circuits and large-scale disconnectivities further point to an involvement of impaired NMDA receptor signaling in the disease.[9]

NMDA receptor function can be modulated by altering the concentrations of the co-agonists D-serine or glycine. The concentration of glycine in the synaptic cleft is regulated by glycine transporters (GlyT). One of the two glycine transporters, GlyT1, is localized at glutamatergic synapses[10] and is physically attached to PSD-95,[11] a protein associated with NMDA receptors. This indicates the role of GlyT1 in regulation of NMDA receptor activity. Preclinical studies have shown beneficial effects of GlyT1 inhibitors in a variety of animal models for schizophrenia addressing the whole spectrum of symptom domains.[12]

Recently, Hoffmann-La Roche announced that two phase III studies of GlyT1 inhibitor RG1678 (bitopertin) did not meet their clinical end points. GlyT1 inhibitors can be differentiated according to their competitive or non-competitive interaction[13] with the glycine binding site on GlyT1 (Figure 1). RG1678 is a non-competitive inhibitor and the lack of clinical effects may be related to its non-competitive binding mode.

Competitive inhibitors may offer potential advantages with respect to their efficacy profile and liability for peripheral side effects. The basis for the potential superiority of substrate-competitive inhibitors is the dependence of the degree of inhibition on the concentration of glycine in the

vicinity of the transporter. While low glycine concentrations would not interfere with the inhibition, high glycine concentrations could displace a competitive inhibitor, and therefore alleviate this block of glycine uptake through GlyT1.

Figure 1. Examples of Non-competitive and Competitive GlyT1 Inhibitors:
Non-competitive Inhibitors:

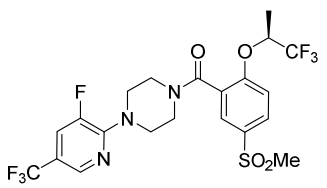

1
RG1678[14]

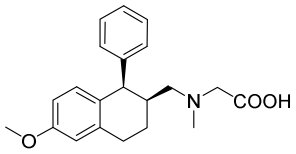

2
Org 25935[15]

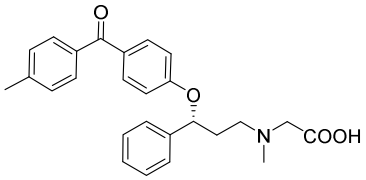

3
(R)-NPTS[16]

Competitive Inhibitors:

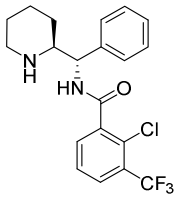

4
SSR504734[17]

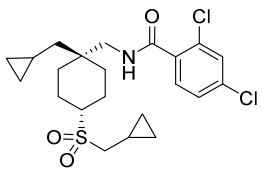

5
DCCCyB[18]

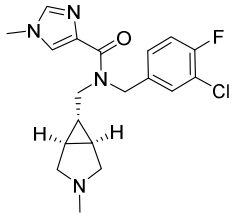

6
PF-03463275[19]

In this paper we report the discovery of aminotetralines and aminochromanes as novel chemotypes of competitive GlyT1 inhibitors. Starting from high-throughput screening (HTS) hit **7** (GlyT1 K_i = 124 nM), SAR studies accompanied by the early assessment of molecular properties and metabolic stability of the synthesized derivatives quickly led to the identification of a sulfonamide side chain attached in the 4-position that significantly increased potency (Table 1). In addition, **7** displayed only moderate selectivity vs. several receptors and transporters (μ-opioid, α_{1A}, dopamine transporter) whereas compound **8** did not show significant receptor binding in the CEREP 75 receptor profile (data not shown).

Table 1. HTS Hit and Early Leads for Optimization

	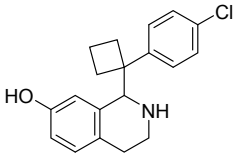 **7**	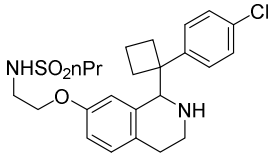 **8**	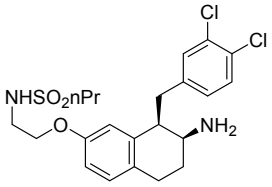 **9**
GlyT1 K_i	124 nM	3.0 nM	35 nM
Mode of action	competitive	competitive	competitive
mClint (r/h)* µL/min/mg	343/130	450/620	17/95
F%** (rat)	< 1%	7%	31%
Brain/Plasma (free)***	n.d.	0.54	0.05
CYP (3A4) inhibition (IC_{50}, µM)****	> 10	0.62	> 10

for details of all parameters see experimental part: determination of ADME parameters; * total clearance of compound in rat and human liver microsomes; ** oral bioavailbility in rat; *** brain/plasma ratio of free drug; **** inhibition of cytochrome P450 3A4 enzyme;

However, **8** was a moderate inhibitor of CYP 3A4. It also suffered from poor oral bioavailability (F%) in rat. We assumed that this is caused by an oxidation/aromatization of the tetrahydroisoquinoline core, which led to suboptimal liver microsomal stability. Among the numerous attempts to prevent this aromatization, moving the nitrogen from an endo- to an exo-cyclic position turned out to be the crucial transformation. This change led to the first aminotetraline compound **9**, which possessed markedly increased liver microsomal stability and ultimately better oral bioavailability while maintaining the GlyT1 potency.

Further studies led to highly potent, selective, drug-like GlyT1 inhibitors, displaying excellent metabolic stability without inhibition of major metabolizing CYP450 enzymes. Throughout SAR

studies we were guided by target occupancy (TO) studies revealing good correlation between unbound brain levels of our GlyT1 inhibitors, corrected by *in vitro* K_i, and the estimated TO. Forebrain homogenates from mice intraperitoneally treated with different doses of a GlyT1 inhibitor, were tested for binding of a GlyT1 radioligand *ex vivo*. Furthermore, our compounds dose-dependently reversed the hyperlocomotion induced in mice by (3*R*,4*R*)-3-amino-1-hydroxy-4-methylpyrrolidin-2-one (L-687,414), which is a known selective and brain-penetrating glycine site NMDA receptor antagonist.

RESULTS AND DISCUSSION

Synthesis. The aminotetraline and aminochromane derivatives examined in this study were prepared as illustrated in Schemes 1 - 6. Scheme 1 shows the initial general synthesis method in which the N-protected aminotetralines were utilized as intermediates for the synthesis of the target sulfonamide containing aminotetralines.

Methoxytetralone **10** was first reacted with benzyl bromides **11** via an enamine to afford benzylated tetralones **12**, which were converted to aminotetralines **13** via reductive amination.[20] In all cases the *cis*-isomer was the major product, which could either be precipitated out directly from the reaction mixture or isolated by flash chromatography. These compounds were first N-protected with ethyl chloroformate in pyridine to aminotetralines **14**, then demethylated with BBr_3 to compounds **15** and subsequently O-alkylated with *tert*-butyl (2-bromoethyl)carbamate in dimethylacetamide in the presence of a base to obtain compounds **16**. Removal of the Boc group produced the intermediates **17**, which were converted to the sulfonamides **19** in the presence of sulfonyl chlorides **18** followed by the removal of the ethyl carbamate with potassium hydroxide in ethanol to afford compounds **20**. The isolation and testing of the minor *trans*-isomers was ultimately abandoned in favor of the *cis*-isomers due to their superior overall profile.

Scheme 1[a]**.** General Synthesis of Aminotetralines

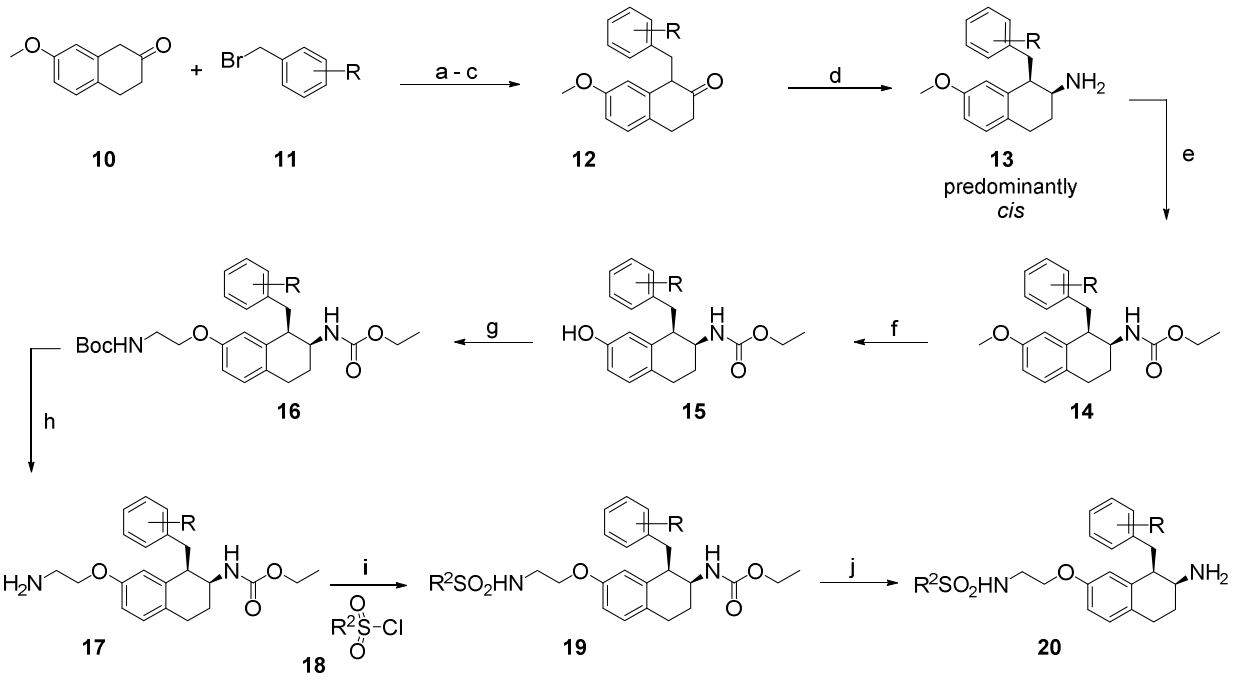

20a: R = 3,4-Cl_2; R^2 = Me
20b: R = 3,4-Cl_2; R^2 = *n*-butyl
20c: R = 3,4-Cl_2; R^2 = *c*-propyl-CH_2
20d: R = 3,4-Cl_2; R^2 = *c*-butyl
20e: R = 3,4-Cl_2; R^2 = 1-Me-pyrrazol-4-yl
20f: R = 3,4-Cl_2; R^2 = 1-Me-imidazole-4-yl
20g: R = 3,4-Cl_2; R^2 = thien-2-yl
20h: R = 3,4-Cl_2; R^2 = phenyl
20i: R = 3-Cl; R^2 = 1-Me-imidazole-4-yl
20j: R = 4-Cl; R^2 = 1-Me-imidazole-4-yl
20k: R = H; R^2 = 1-Me-imidazole-4-yl
20l: R = 2-Cl; R^2 = 1-Me-imidazole-4-yl
20m: R = 5-Cl, 3-F; R^2 = 1-Me-imidazole-4-yl
20n: R = 3 CF_3; R^2 = 1-Me-imidazole-4-yl

[a] Reagents and conditions. (a) Pyrolidine, MeOH, RT, 1 h (b) **11**, MeCN, overnight; (c) MeOH/DCM/H_2O 1:1:1, glacial acid, overnight; (d) $NaCNBH_3$, NH_4OAc, MeOH, RT, 4 d; (e) Ethylchloroformiate, pyridine, RT, overnight; (f) BBr_3, DCM, -10°C, 2 h (g) *tert*-butyl (2-bromoethyl)carbamate, NaH, DMA, RT, 3 d; (h) HCl, *i*PrOH, RT, overnight (i) **18**, DMAP, RT, overnight (j) KOH in EtOH, RT, 2 h.

The synthesis of enantiomerically pure aminotetralines is shown in Scheme 2. Tetralone **12** was first converted to the propionenamide **21** which was further transformed to compound **(1*R*,2*S*)-22** by enantioselective hydrogenation mediated by chlorocyclooctadiene rhodium(I) dimer in the presence of (S)-1-[(R_P)-2-(Di-1-naphtylphosphino)ferrocenyl]ethyldi-tert.-butylphosphine (Josiphos SL-J216-2).[21-23] In all tested cases the observed enantiomeric excess (ee) was higher than 90% which could be further increased to ee > 99% by recrystallization as determined by HPLC using an Agilent 1100 HPLC (samples run on Chiralpak AD-H, for further details see experimental section). Such a process was also exploited successfully in process scale synthesis of these chiral compounds. Finally, the propionamide was hydrolyzed in the presence of

sulfuric acid to obtain **(1*R*,2*S*)-13** (R=H). The absolute configuration was assigned by single crystal x-ray analysis of the (S)-(+)-mandelic acid salt of amine **(1*R*,2*S*)-13** (R=H). Demethylation afforded hydroxy compound **(7*S*, 8*R*)-23**, which was subsequently alkylated with 1,3-dibromopropane or 1,4-dibromobutane to give compounds **(7*S*, 8*R*)-24**. Aminotetraline derivatives **(7*S*,8*R*)-25** were then obtained by O-alkylation with *tert*-butyl (2-bromoethyl)carbamate in dimethylacetamide in the presence of a base. Removal of the Boc group produced **(7*S*,8*R*)-26**, which were further converted to final compounds **(7*S*, 8*R*)-27** carrying an azetidine or pyrrolidine residue.

Scheme 2[a]. Synthesis of Enantiopure Aminotetralines

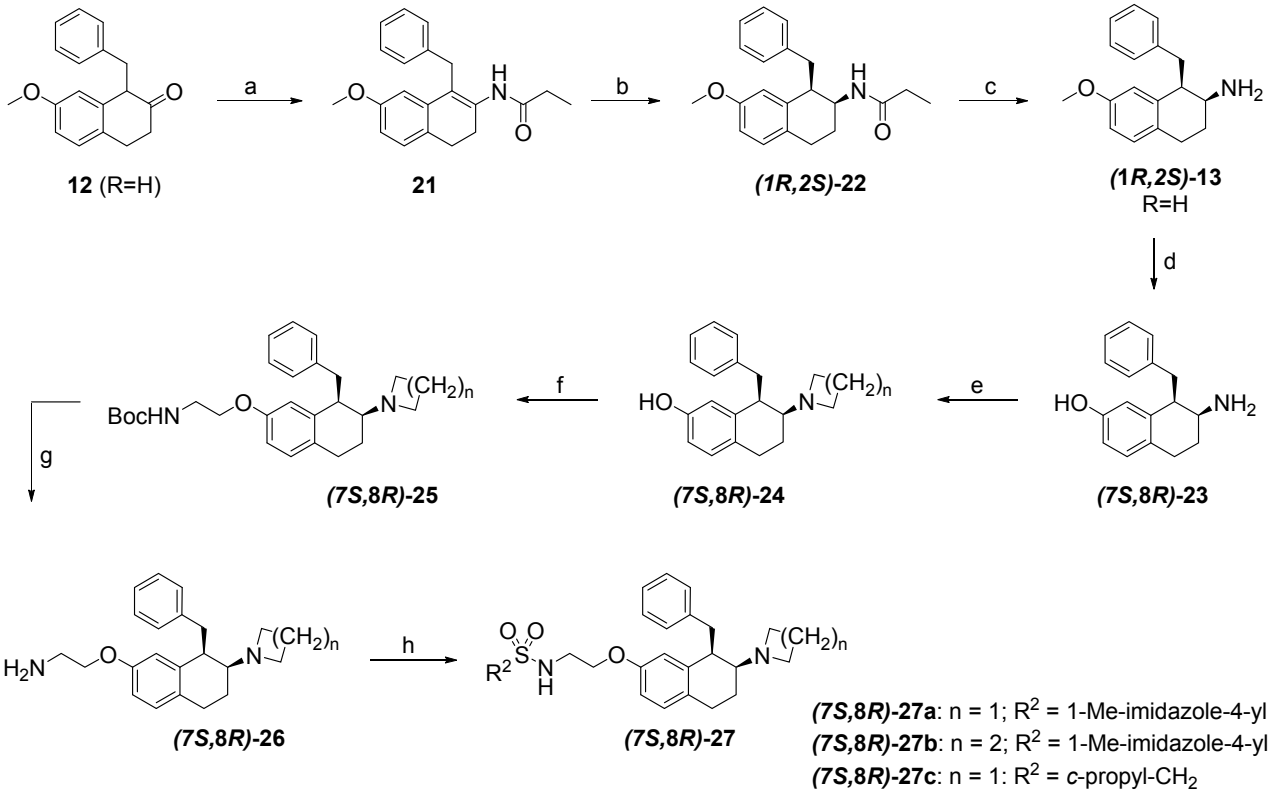

[a] Reagents and conditions. (a) Propionamide, pTsOH, toluene, reflux, 5 d; (b) Josiphos SL-J216-2, chlorocyclooctadiene Rh (I) dimer, H_2, methanol, 50-55°C, 4 bar, 40 h; (c) Sulfuric acid, acetic acid / water, reflux, 68 h (d) HBr, acetic acid, 110°C, 1.5 h (e) Alkyl dibromide, *N*,*N* diisopropylethylamine, MeCN, overnight; (f) *tert*-Butyl (2-bromoethyl)carbamate, NaH, DMA, RT, 3 d; (g) HCl, *i*PrOH, RT, overnight (h) R^2SO_2Cl, DMAP, RT, overnight.

Alternatively, chiral resolution of the racemates of final compounds or intermediates by preparative HPLC or preparative SFC can be achieved (see experimental part for further details). The general synthesis method for the aminochromanes on the other hand started with 6-methoxychroman-4-one **28** as shown in Scheme 2. Transformation to **29** and a subsequent Neber-rearrangement afforded amino ketone **30**,[24] which was N-protected to give **31** and further reacted with benzylmagnesium chloride, to produce compound **32** after acidic workup.

Scheme 3[a]. Synthesis of Aminochromane Derivatives **36**

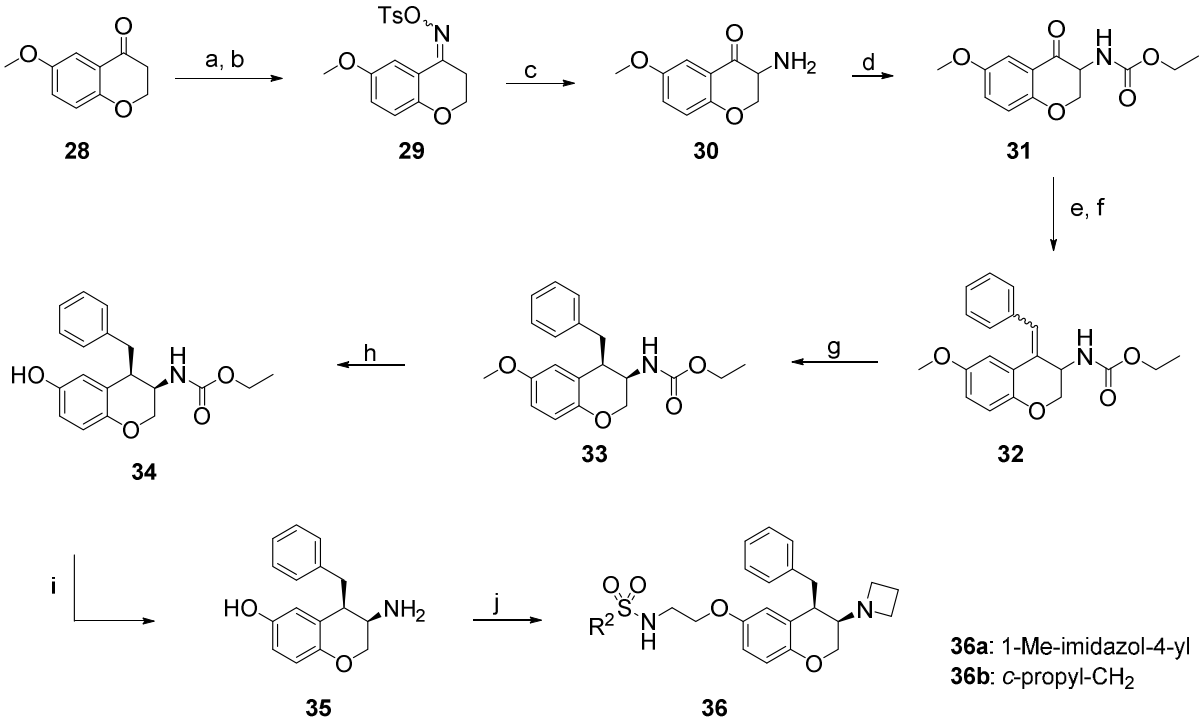

[a] Reagents and conditions. (a) NH_2OH, EtOH/H_2O, 70°C, 1.5 h; (b) TsCl, pyridine, 0°C to RT, overnight; (c) NaOEt, toluene/dichloromethane, 0°C to RT, overnight; (d) Ethylchloroformiate, THF, DIPEA, 0°C to RT, 0.5 h; (e) Benzylmagnesium chloride , THF, 0°C, 0.5 h; (f) half concentrated HCl, 100°C, 1 h; (g) Pd/C, NH_4CO_2, EtOH/H_2O, 75°C, 1 h; (h) BBr_3, DCM, 0°C, 2 h; (i) EtOH, KOH 20%, 70°C, overnight (j) See scheme 2 steps (7*S*,8*R*)-**24** through (7*S*,8*R*)-**27**.

Intermediate **33** was then prepared by hydrogenation of the benzylidene compound, which was demethylated to **34** with BBr_3 and deprotected under basic conditions affording **35.** Further conversion to the target compounds **36** was achieved following the protocol described in Scheme 2 for compounds **27** which involves the subsequent steps: formation of azetidine with 1,3-

dibromopropane, O-alkylation with *tert*-butyl (2-bromoethyl)carbamate in dimethylacetamide in the presence of a base, removal of the Boc group, and conversion to the sulfonamides **36**.

Scheme 4 shows the general synthesis of compounds with a truncated side chain and an azetidine instead of a free amino group. Hydroxytetraline **37** was first converted to the triflate **38** which was further transformed to nitrile **39** by Pd-mediated cross couplings. Deprotection of the amino group produced compound **40** which were then converted to the azetidine **41** by alkylation with 1,3-dibromopropane. Subsequent hydrogenation of the nitrile group afforded free amine **42**, which were converted to the sulfonamide **43** using the corresponding sulfonyl chlorides in the presence of DMAP.

Scheme 4[a]. Synthesis of Aminotetralines with Short Sulfonamide Side Chain

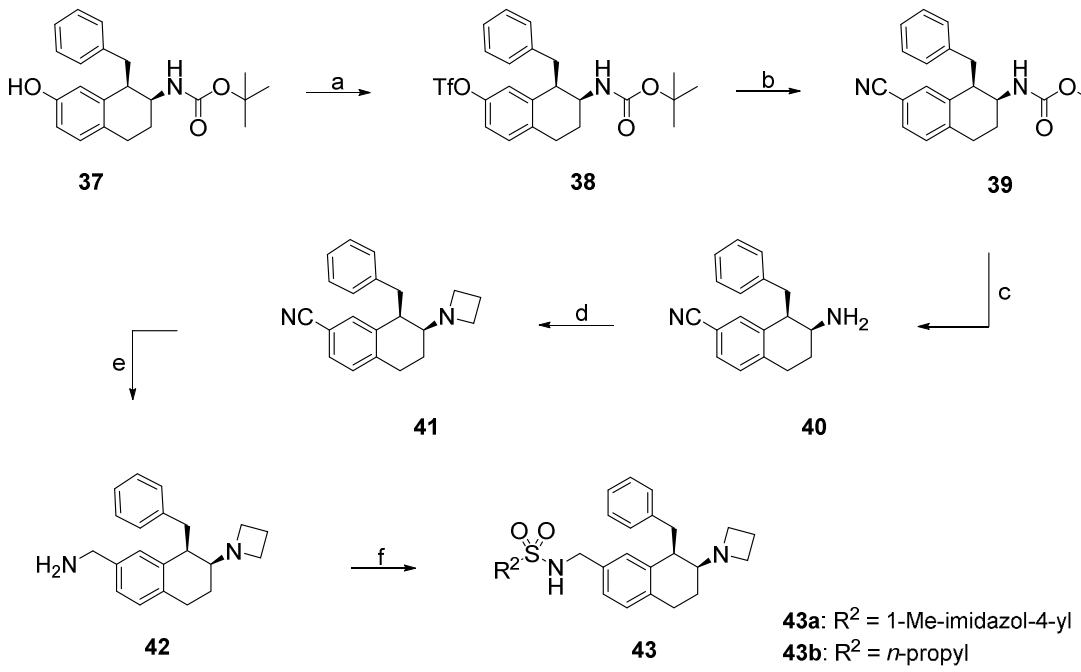

[a] Reagents and conditions. (a) Tf_2O, DCM, 0°C, 0.5 h; (b) $Zn(CN)_2$, $Pd_2(dba)_3$, dppf, DMF, 120°C, 1 h; (c) R = *t*-Bu: TFA, DCM, RT, overnight; R = Et: TMS-I, $CHCl_3$, 3.5 h, reflux; (d) 1,3-Dibromopropane, NEt_3, MeCN, µW, 120°C; (e) H_2, Raney nickel, 1 bar, MeOH, 48 h, RT; (f) R^2SO_2Cl, DMAP, RT, overnight.

Mono-N-alkylated aminotetralines as shown in scheme 5 were prepared starting from the primary amine **20k** which was converted to amide **47** or from intermediates **19** or **45**. Subsequent reduction with $LiAlH_4$ or BH_3SMe_2 affords the desired compounds **44**, **46** and **48**.

Scheme 5[a]: Synthesis of N-alkylated Aminotetralines

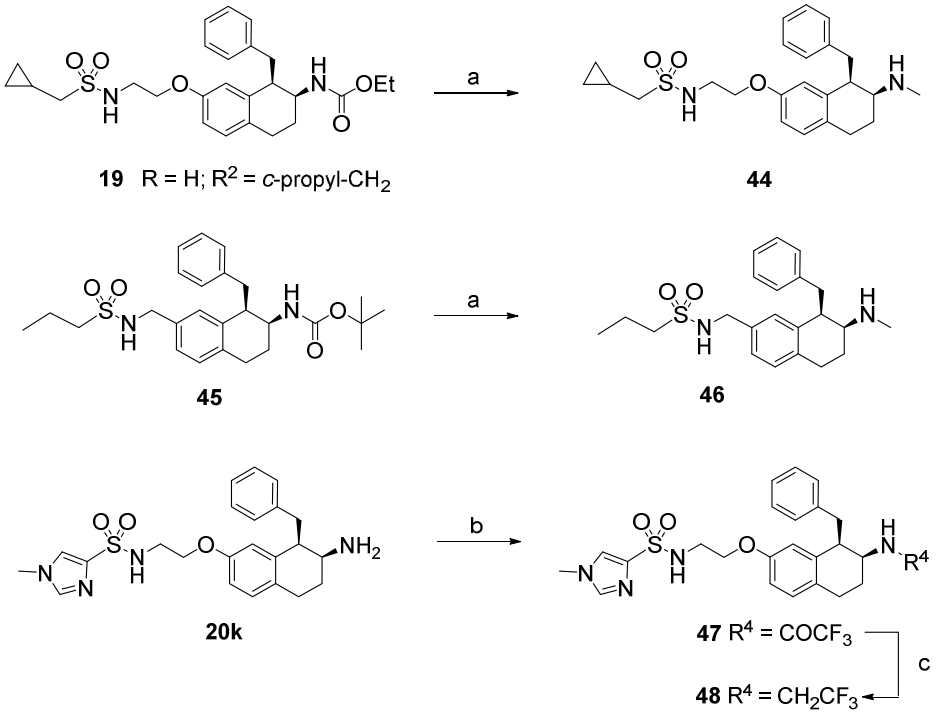

[a] Reagents and conditions. (a) $LiAlH_4$ (1M in THF), THF, reflux, 3h; (b) Trifluoroacetic anhydride, NEt_3, THF, RT, overnight (c) BH_3SMe_2 (2M in THF), THF, 60°C, overnight

Scheme 6 depicts the synthesis of aminotetralines and aminochromanes carrying a rigidified side chain. Triflate **49,** was converted to the Boc-protected intermediates **50** and **52** by Pd-mediated cross-couplings. Deprotection of the amino group and subsequent conversion to the sulfonamide afforded final compounds **51** and **53**.

Scheme 6[a]. Synthesis of Aminotetralines and Chromanes with Rigidified Side Chains

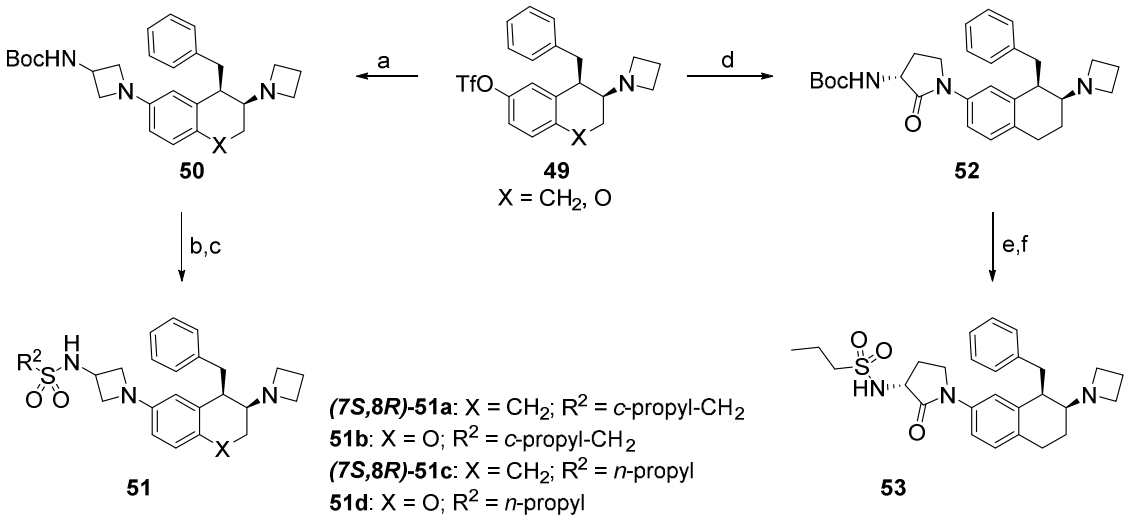

[a] Reagents and conditions. (a) $Pd(OAc)_2$, XPhos, Cs_2CO_3, 3-((*tert*-butoxycarbonyl)amino)azetidin-1-ium chloride, toluene, 115°C, 1.5 h; (c) TFA, DCM, RT, overnight; (d) R^2SO_2Cl, DMAP, RT, overnight (d) (*R*)-*tert*-Butyl (2-oxopyrrolidin-3-yl)carbamate; BrettPhos, $[PdCl(allyl)]_2$, Cs_2CO_3, toluene, 140°C, 2 h, µW; (e) TFA, DCM, RT, overnight; (f) 1-Propanesulfonyl chloride, DMAP, DCM, RT, overnight.

Structure activity relationships: Early SAR studies aimed at maximizing GlyT1 potency and further improvement of liver microsomal stability (rat/human). Liver microsomal metabolism studies indicated that the *n*-propyl residue of sulfonamide **9** was prone to oxidation and therefore a metabolic hotspot. A targeted library of heterocyclic and alkyl sulfonamides was synthesized by sulfonamide couplings with the corresponding sulfonyl chlorides (Scheme 1). In comparison to related derivatives **9**, **20a, 20b** and **20d** bearing sulfonamide moieties of similar size, the cyclopropyl methyl compound **20c** displayed improved potency. However, liver microsomal stability was not improved, resulting in a dose of 14 mg/kg to achieve 50% TO in mice (i.p. dosing). Methyl pyrazole **20e** showed good potency but with similar turnover in rat liver microsomes compared to compound **9**. Methyl imidazole **20f** emerged as a lead for further optimization, showing improved potency and lower microsomal turnover relative to compound **9**. Replacing the imidazole or pyrrazole moiety by thienyl **20g** or phenyl **20h** led in turn to compounds with much higher K_is. Despite high potency, both GlyT1 inhibitors, **20e** and **20f**

required a high dose to achieve half maximal TO, probably due to low brain availability (**20e**: unbound, $C_{max,brain}$ = 0.2 nM at 2 mg/kg i.p.). Surprisingly the same trend with respect to potency was also published for a series of GlyT1 inhibitors by Merck despite a very different core structure.[25]

Table 2. *In Vitro* Inhibitory Activity of **9**, **20a-h** at hGlyT1 and their Metabolic Stability

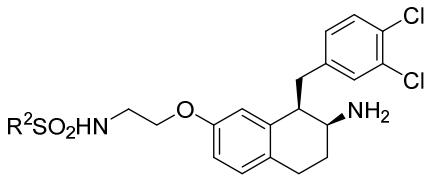

Compound	R^2	K_i [nM] hGlyT1	mClint* [µL/min/mg] rat / human	ED_{50} est. TO (mice) [mg/kg i.p.]	clogP / TPSA
9	*n*-Propyl	35	17 / 95	n.d.	5.4 / 81
20a	Me	141	39 / 25	n.d.	4.4 / 81
20b	*n*-Butyl	136	35 /173	n.d.	6.0 / 81
20c		5.7	25 / 92	14	5.4 / 81
20d		32	49 / 55	n.d.	5.3 / 81
20e	1-Me-pyrrazol-4-yl	1.2	49 / 44	> 20	4.7 / 99
20f	1-Me-imidazole-4-yl	2.6	10 / 36	> 20	5.0 / 99
20g	Thien-2-yl	163	95 / 99	n.d.	5.9 / 81
20h	Phenyl	660	40 / 78	n.d.	6.0 / 81

K_i values and estimated ED_{50} for *in vivo* target occupancy (ED_{50} est. TO) was assessed as described in the experimental part; * total clearance of compound in rat and human liver microsomes (see experimental section)

GlyT1 inhibitors depicted in Table 2 have a clogP in the range of 4.4 to 6 and a TPSA in the range of 81 to 99. Based on improved potency of **20f**, we focused next on the optimization of the benzyl moiety by reducing the lipophilicity, while keeping the 1-Me-imidazole-4-sulfonyl functionality in place. Table 3 highlights selected compounds from this effort (clogP 3.6 to 5.1).

High affinities were obtained with analogues carrying substituents in the 3-, 4-, or 5-position of the benzyl residue (entries **20i**, **20j** and **20m**, **20n**), whereas substitution in the 2-position (**20l**) afforded compounds with somewhat lower potency. However compound **20k** carrying an unsubstituted phenyl ring displayed one of the best affinities (K_i hGlyT1 = 3.6 nM) combined with a good liver microsomal stability (mClint [µL/min/mg]: h < 23; r < 23). The unsubstituted benzyl side at the aminotetraline core was therefore retained for further optimization.

Compounds **20f** and **20i** of table 3 still displayed low brain availability which led to an unfavorable ED_{50} in our *ex vivo* binding assay. The favorable physicochemical space (topological polar surface area (TPSA) = 45, clogP = 2.8, number of hydrogen bond donors (#HBD) = 1, pK_a = 8.4, MW 305), for CNS drugs has been described in numerous publications.[26-28]

Table 3. *In Vitro* Inhibitory Activity of Different Benzyl Derivatives **20f**, **20i-20n** at hGlyT1

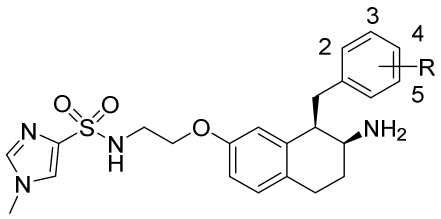

Compound	R	K_i [nM] hGlyT1	ED_{50} est. TO (mice) [mg/kg]	clogP / TPSA
20f	3,4-Cl_2	2.6	> 20	5.0 / 99
20i	3-Cl	1.5	15	4.3 / 99
20j	4-Cl	1.1	n.d.	4.3 / 99
20k	H	3.6	n.d.	3.6 / 99
20l	2-Cl	75	n.d.	4.3 / 99
20m	5-Cl, 3-F	1.2	n.d.	4.5 / 99
20n	3-CF_3	0.8	n.d.	4.5 / 99

K_i values and estimated ED_{50} for *in vivo* target occupancy (ED_{50} est. TO) was assessed as described in the experimental part

Compounds within this space have a higher likelihood of being brain penetrant and displaying a benign safety profile. Reducing the TPSA (TPSA = 99 for all compounds in table 3) and the number of hydrogen bond donors (#HBD = 3 for all compounds in table 3) was therefore the next step.

A reduction of HBDs can be achieved by elimination of protic hydrogen atoms, whereas TPSA can be reduced most easily by replacing nitrogen, oxygen or protic hydrogen atoms by carbon atoms, and the number of rotatable bonds by rigidification of the sulfonamide bearing side chain. An iterative approach was employed to rapidly develop SAR. Table 4 displays selected compounds resulting from these extensive studies, in which TPSA and number of HBDs were reduced stepwise.

Table 4. *In Vitro* Inhibitory Activity of Different Amine Derivatives at hGlyT1

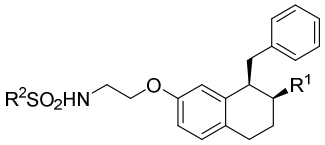

20k, 27a-c, 44

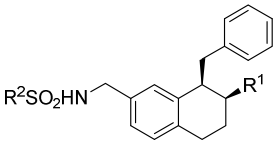

43a, 46

Compound	R^2	R^1	K_i [nM] hGlyT1	TPSA [Å^2]	HBD	ED_{50} est. TO (mice) [mg/kg]
20k		NH_2	3.6	99	3	n.d.
(7*S*,8*R*)-27a	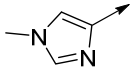		0.8	76	1	1.4
(7*S*,8*R*)-27b			1.2	76	1	1.6
(7*S*,8*R*)-27c			2.6	59	1	0.5
(7*S*,8*R*)-44		NHMe	1.2	67	2	1.4
43a	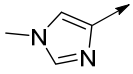		3.0	63	1	1.8
46	*n*-Propyl	NHMe	9.5	58	2	2.0

K_i values and estimated ED_{50} for *in vivo* target occupancy (ED_{50} est. TO) was assessed as described in the experimental part

As assumed these variations led to compounds with improved brain availability, demonstrated by low single digit doses to achieve 50% TO in mice. Compound (***7S,8R***)-**27c** combines low TPSA with the least number of HBDs and also exhibited an good brain to plasma drug concentration ratio of 0.8 (unbound, $C_{max,brain}$ = 9.9 nM at 2 mg/kg i.p.) in rat and achieved an ED_{50} of 0.5 mg/kg (i.p.) in our *ex vivo* binding assay.

(**7*S*,8*R***)-**27c** showed relatively high liver microsomal clearance (mClint [µL/min/mg]: h = 113; r = 137), which could be a reason for its low oral bioavailability in rat ($F_{p.o.}$ = 8%). Additionally, it proved to be a very potent hERG inhibitor with an IC_{50} of 80 nM. Compared to (**7*S*,8*R***)-**27c**, compound (**7*S*,8*R***)-**44** has a higher TPSA (67Å^2) and 2 HBDs but still achieved a good unbound drug concentration in the brain ($C_{max,brain}$ = 2.3 nM at 2 mg/kg i.p.) resulting in an ED_{50} of 1.4 mg/kg in the *ex vivo* binding assay. Liver microsomal clearance was still an issue but oral bioavailability in rat was 22%. Compound **46** represents an analogue with a shorter sulfonamide side chain. It carries a methylated amino group leading ultimately to an ED_{50} of 2.0 mg/kg in the *ex vivo* binding assay. Further reduction of the number of HBDs by introduction of an azetidine afforded **47a**, which achieved again a good unbound drug concentration in the brain ($C_{max,brain}$ = 13 nM at 2 mg/kg i.p) and an ED_{50} of 1.8 mg/kg in the *ex vivo* assay despite the replacement of the *n*-propyl group by a more polar imidazole moiety. In addition compound **43a** displayed good oral bioavailability in preclinical species ($F_{p.o.}$ = 51% in rat and 75% in dog).

Compounds (**7*S*,8*R***)-**27a** and (**7*S*,8*R***)-**27b** showed the best overall profile. Both proved to be very selective with no significant receptor binding in the CEREP profile (75 receptors tested at 10 µM) with an ED_{50} of 1.4 mg/kg and 1.6 mg/kg respectively in the *ex vivo* binding assay. The unbound drug concentration in brain was determined to be 2 nM for both, (**7*S*,8*R***)-**27a** and (**7*S*,8*R***)-**27b** at a dose of 1 mg/kg i.p. Liver microsomal stability was moderate without inhibition of major metabolizing CYP450 enzymes and oral bioavailability in preclinical species was 17%

(rat) / 75% (dog) for (**7*S*,8*R*)-27a** and 29% (rat) / 49% (dog) for (**7*S*,8*R*)-27b**. In addition both GlyT1 inhibitors displayed an excellent solubility in water of more than 1 mg/mL, and high permeability in the MDCK assay of $22 \cdot 10^{-6}$ cm/s (**7*S*,8*R*)-27a** and $17 \cdot 10^{-6}$ cm/s (**7*S*,8*R*)-27b** indicating BCS I like properties.

In order to study the mode of inhibition of the advanced GlyT1 inhibitors, the functional inhibition was studied with two different glycine concentrations, 10 µM and 3000 µM.[13] The K_i of RG1678 for GlyT1 was 47 nM and for **(7*S*,8*R*)-27a 0**.8 nM as determined in our ligand binding assay. 300 nM RG1678 inhibited the 10 µM glycine current by 67 ± 8% (n=4), and blocked the current of 3000 µM glycine by 95 ± 1% (n=6). In contrast, **(7*S*,8*R*)-27a** demonstrated inhibition of 97 ± 1% (n=4) at 10 µM and only 39 ± 3% (n=5) at 3000 µM glycine (Fig. 2). These results indicate that while RG1678 appears to be a non-competitive inhibitor of GlyT1c, **(7*S*,8*R*)-27a** competitively inhibits glycine transport.

Figure 2. Oocyte Experiments with RG1678 (**1**) and **(7*S*,8*R*)-27a**

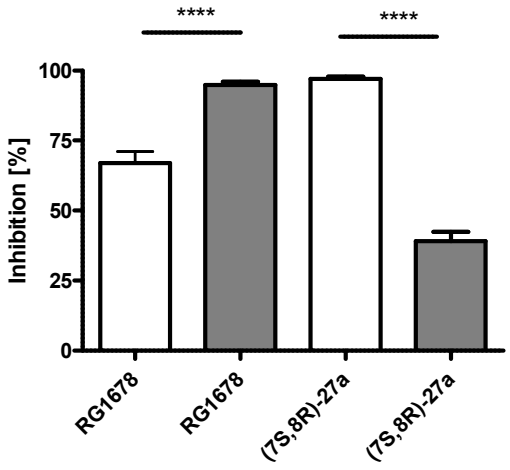

Surmountability of GlyT1 inhibitors. Oocytes expressing GlyT1c were stimulated with 10 µM (open bars) or 3000 µM (dark bars) glycine to induce a current through the transporter. 300 nM RG1678 (left) or 300 nM **(7*S*,8*R*)-27a** (right) were added to the glycine solution, and the inhibition of the current calculated. Data are represented as mean +/- SD, N>4, **** $p<0.0001$.

Furthermore, compound (**7*S*,8*R*)-27a** dose-dependently reversed L-687,414-induced hyperlocomotion in mice (Figure 3).[29] L-687,414 ((3*R*,4*R*)-3-amino-1-hydroxy-4-methylpyrrolidin-2-one)[30] is a known selective and brain-penetrant glycine site NMDA receptor antagonist. This behavioral effect was also described with the non-competitive GlyT1 inhibitors RG1678 and the sarcosine-based compound Org25935 (**2**), and likely results from the increased extracellular level of glycine in the brain through GylT1 transport inhibition. This increased glycine level subsequently displaces the NMDA glycine-site antagonist. (**7*S*,8*R*)-27a** reached 50% inhibition of L-687,414-induced hyperlocomotion at a dose of 0.8 mg/kg after i.p. administration, which is comparable to the dose necessary to achieve 50% TO.

Figure 3. Reversal of L-687,414-induced Hyperlocomotion by Compound (**7*S*,8*R*)-27a**

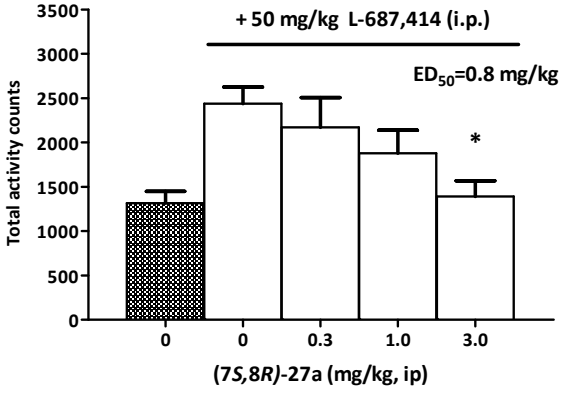

Non-habituated mice were injected i.p. with (**7*S*,8*R*)-27a** or its vehicle 120 min prior to test. 15 min prior to the test, animals were then treated with 50 mg/kg (i.p.) of L-687,414 or its vehicle and the locomotor activity was measured for 60 min. Wilcoxon-Mann-Whitney test revealed a significant stimulatory effect of L-687,414 (Mann Whitney test, $p=0.0006$). (**7*S*,8*R*)-27a** dose dependently reduced the L-687,414-induced hyperlocomotion reaching statistical significance at 3 mg/kg (Dunn's multiple comparisons test, $*p<0.05$). Data are shown as mean ± SEM for n=8 mice per group.

However, a high efflux ratio (ER) in the MDR1 transwell assay was observed ((**7*S*,8*R*)-27a**: ER = 12; (**7*S*,8*R*)-27b**: ER = 7.2). Consistently, in a subsequent study with (**7*S*,8*R*)-27b** in MDRIa/b +/+ and -/- mice, the brain to blood ratio of MDR1a/b -/- mice was 26-fold higher than in the MDR1a/b +/+ mice. This strengthens our finding in the *in vitro* studies and suggest that compound (**7*S*,8*R*)-27b** is likely an *in vivo* substrate of the efflux transporter P-glycoprotein. These results sparked the initialization of a second round of optimization.

We first examined the effect of reducing TPSA and the number of hydrogen bond donors on lowering ER.[31] Following this strategy, we identified compound **27c**, with a superior ER of 1.6. However, the compound proved to be a very potent inhibitor of hERG (IC_{50}: 80 nM). As a second approach, we speculated that a reduction of basicity could positively influence the ER,[32-34] since compound **48,** a close analogue of (**7*S*,8*R*)-27a,** with a calculated pKa of 5.6, displayed an ER of only 1.4. As shown in table 5, inhibition of GlyT1 was still moderate K_i = 69 nM, but liver microsomal clearance was too high to allow further development. Since the same effect on microsomal stability was also seen for additional compounds with fluorine containing alkyl side chains, we suspended these variations and instead pursued an exchange of our central core to the amino chromanes. The amino group of this scaffold has a calculated pKa value of 8.0 and offers the possibility to prepare compounds, which have a lower degree of protonation at neutral pH. Indeed, compound **36a** displayed a reduced ER of 3.5, compared to (**7*S*,8*R*)-27a** (ER = 12). In general, amino chromanes were well tolerated in rodents, but the resulting compounds often displayed a higher liver microsomal clearance compared to the aminotetralines. In summary, up to this point both series, aminotetralines and -chromanes had suboptimal properties, but rigidification of the sulfonamide bearing side chain could potentially reduce liabilities. A number

of derivatives with different linkers were synthesized and studied. The summary of these approaches is shown in Table 6 for some selected compounds.

Table 5. Derivatives of Compound **20k**: Calculated pKa and Influence on ER

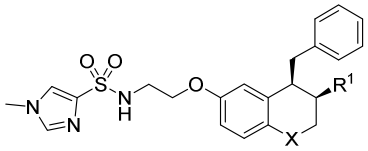

Compound	R^1	X	K_i [nM] hGlyT1	mClint (h / r) [µL/min/mg]		pKa (calc.)	ER
(7*S*,8*R*)-27a		CH_2	0.8	10	55	9.4	12
(3*R*,4*R*)-36a		O	3.3	37	277	8.0	3.5
48	$NHCH_2CF_3$	CH_2	69	125	103	5.6	1.4

K_i values and estimated ED_{50} for *in vivo* target occupancy (ED_{50} est. TO) was assessed as described in the experimental part

Compared to (**7*S*,8*R*)-27c**, the potency of compound **36b** is much reduced and liver microsomal clearance is higher**.** Shortening of the ethanol amino side chain to a methylene amino linker afforded compound **43b**, however, also this derivative displayed lower potency. Compounds (**7*S*,8*R*)-51a – (3*R*,4*R*)-51d** carry an azetidine linker, which had the highest impact on all desired parameters in both series. This side chain retains excellent K_i, shows improved microsomal stability and reduced P-gp substrate liability, combined with low hERG inhibition, validating our hypothesis that lowering pKa of the central core and/or rigidification of the linker would lead to improved *in vitro* parameters. In addition, it could be shown that a more polar pyrrolidinone linker was tolerated giving equally potent, metabolically stable compound **N-(*R*)-(7*S*,8*R*)-53** (clogP 3.5, TPSA 70) with low ER. Compound (**7*S*,8*R*)-51a** is a selective and potent competitive GlyT1 inhibitor with no significant receptor binding in the CEREP profile (75 receptors tested at

10 μM). It has an oral bioavailability in rat comparable to that of compound (**7*S*,8*R*)-27a** (F_{po} = 25%) but achieved unbound drug concentrations of 18.7 nM in the brain at (2 mg/kg i.p.). Assuming dose linearity, a drug concentration of 0.9 nM (equivalent to K_i) is achieved in brain at doses in the range of 0.2 mg/kg. Indeed a subsequent *ex vivo* TO study, revealed an estimated ED_{50} of 0.2 mg/kg for compound (**7*S*,8*R*)-51a,** which correlates well with the predicted value. A complete evaluation of free brain levels vs. K_i in all TO studies confirms this further (Figure 4).

Table 6. *In Vitro* Inhibitory Activity of Aminotetralines and Aminochromanes with Different Moieties R^4 at hGlyT1

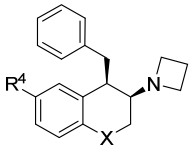

			K_i [nM]	mClint (h / r)			hERG
compound	R^4	X	hGlyT1	[μL/min/mg]		ER	IC_{50} [μM]
(7*S*,8*R*)-27a	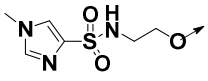	CH_2	0.8	10	55	12	15
(3*R*,4*R*)-36a		O	3.3	38	277	3.5	n.d.
(7*S*,8*R*)-27c	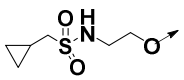	CH_2	2.6	113	137	1.6	0.08
36b		O	239	239	940	n.d.	n.d.
43b	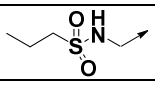	CH_2	71	122	302	n.d.	n.d.
(7*S*,8*R*)-51a	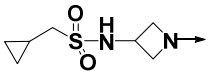	CH_2	0.9	< 23	85	1.7	4.4
51b		O	18	< 23	130	1.0	11.4
(7*S*,8*R*)-51c	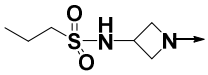	CH_2	2.6	< 23	42	1.4	6.8
51d		O	44	< 23	66	0.9	n.d.
***N*-(*R*), (7*S*,8*R*)-53**	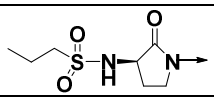	CH_2	28	< 23	33	1.6	4.5

K_i values and estimated ED_{50} for *in vivo* target occupancy (ED_{50} est. TO) was assessed as described in the experimental part

The receptor occupancy from *ex vivo* binding was determined as a function of the free brain concentration, over a dose range and the free brain EC_{50} values were calculated for each compound by fitting to an E_{max} model. Figure 4 shows the correlation of the free brain EC_{50} and the *in vitro* K_i for the available dataset. The correlation is very good (Pearson r = 0.86; r^2 = 0.73), indicating that the *in vitro* K_i value is a relevant measure to predict the receptor occupancy *in vivo*, when considering the free concentration of the compound in the brain.

Figure 4. Correlation between the Free Brain EC_{50} Target Occupancy and *in vitro* K_i

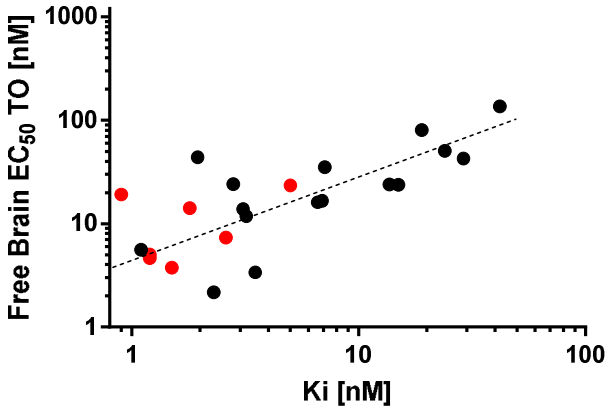

The apparent brain EC_{50} values were determined by curve fitting from the receptor occupancy curve over the free concentration/K_i, using the brain concentrations corrected for the fraction unbound in brain ($f_{u,brain}$). The dashed line represents the linear curve fit of the data set (Pearson r = 0.86; r^2 = 0.73). Red symbols represent the compounds described in detail in the chemistry section of this publication.

The relevance of the development of competitive over non-competitive inhibitors for GlyT1 has been discussed in the literature.[13] The alleviation of GlyT1 inhibition through competitive inhibitors by high glycine could make it possible to eliminate high glycine concentrations

associated with efficacy-compromising and potentially toxic effects, within the glutamatergic synapse, but more importantly also in inhibitory glycinergic synapses, while still allowing a moderate increase of glycine in order to enhance the activity of the NMDA receptor. It is known that different glycine levels are required for the activation of NMDA receptors (efficacy mediating target) and the induction of unwanted effects (efficacy compromising effects or peripheral side effects), which are in part mediated by the strychnine-sensitive glycine receptor. NMDA receptors are activated by low glycine concentrations, as indicated by the K_d of glycine for the modulatory site of NMDA receptors in the low μM range.[35,36] Much higher concentrations of glycine are required to activate strychnine-sensitive glycine receptors as suggested by the lower affinity of glycine for these receptors with K_d values in the high μM range.[37,38] Activation of strychnine-sensitive glycine receptors has been shown to suppress long-term potentiation (LTP),[39] a NMDA receptor mediated effect induced by lower concentrations of glycine. This could explain the bell-shaped concentration-response curve of LTP induction mediated by the non-competitive inhibitor RG1678 (**1**).[40] Internalization of NMDA receptors is a further mechanism which could compromise NMDA receptor activity at high glycine levels. Internalization occurs at glycine concentrations in the range of 40 μM,[41] again much higher than the concentration required for NMDA receptor activation.

Since high concentrations of glycine displace competitive inhibitors from their binding side, these efficacy-compromising effects may be less pronounced in the case of a competitive inhibitor as compared to a non-competitive inhibitor. This displacement is particularly relevant in glycinergic synapses, where the range of concentrations of glycine is large. In that case, functioning of GlyT1 transport in these synapses by competition of the inhibitor by high synaptic glycine concentrations can lead to an alleviation of the inhibition and a normalization of synaptic functioning of these inhibitory synapses.

Compared to extracellular glycine concentrations in the brain, peripheral extracellular glycine levels are much higher.[42] Therefore the liability for peripheral side effects such as a reduced heme synthesis,[43] which are due to blockade of glycine uptake into peripheral cells, should be significantly lower for competitive inhibitors.

The described function of competitive GlyT1 inhibitors may lead to less central and peripheral side-effects and would make competitive inhibitors more promising drug candidates compared to non-competitive GlyT1 blockers. This hypothesis will need to be further substantiated by elaborate pharmacological experiments.

CONCLUSION

In summary, chemical modifications of the original tetrahydroquinoline core led to the discovery of aminotetralines as new series of GlyT1 inhibitors. We successfully improved potency and brain availability and identified compound (**7*S*,8*R***)-**27a**[44] as a highly potent and selective GlyT1 inhibitor, exhibiting excellent pharmacokinetic properties. These resulted in low doses to achieve half maximum TO and high efficacy in the L-687,414-induced hyperlocomotion assay. Further SAR studies revealed compound (**7*S*,8*R***)-**51a**[45,46] displaying further improvements over (**7*S*,8*R***)-**27a** regarding the ER and ex vitro binding efficacy. The biological characterization of these compounds will be reported in further detail in forthcoming publications.

EXPERIMENTAL SECTION

Chemistry. All commercially available chemicals and solvents were used without further purification. In general, reaction mixtures were magnetically stirred at the respective temperature under nitrogen atmosphere. Organic solutions were concentrated under reduced pressure using a Buechi rotovap. Reactions under microwave irradiation conditions were carried out in a Biotage Initiator EXP instrument. Normal phase chromatography was performed on an ISCO CombiFlash

Companion MPLC system using RediSep prepacked columns with silica, and reverse phase chromatography was performed using Chromabond C18 cartridges. Reactions were monitored by thin layer chromatography using HPTLC Silicagel 60 F254 plates from Merck KGaA and were visualized using 254 nm ultraviolet light and/or exposure to silica gel impregnated with iodine. Optical rotations were obtained on a PerkinElmer polarimeter 341. All new compounds gave satisfactory ^{1}H NMR and LC/MS. On the basis of LCMS, all final compounds were >95% pure unless otherwise noted. NMR spectra were obtained on a Bruker Avance I 400 MHz or Avance III 500 or 600 MHz NMR spectrometer using residual signal of deuterated NMR solvent as internal reference; chemical shifts for protons are reported in a parts per million scale downfield from tetramethylsilane. Analytical LCMS data were obtained using an Agilent 1100 series HPLC system with DAD and SQ mass spectrometer with ESI in positive mode and a scan range of 100−700 amu. Samples were run on a Chromasil 80 ODS-7pH column 4μm, 40 mm × 2 mm; gradient elution 5−100% B over 10 min; solvent A, H_2O/0.1% TFA; solvent B, MeCN/0.1% TFA; flow rate, 0.5 mL/min; temperature, 60°C. Chiral compounds were analyzed by chiral HPLC using an Agilent 1100 HPLC with samples run on Chiralpak AD-H 4.6 mmID × 250 mm; 5 μm; with *n*-hexane/EtOH/MeOH 20/40/40 as mobile phase; flow rate, 0.6 mL/min and detection at 300 nm wavelength. Chemical names were generated using ChemDraw Professional 15.0 (PerkinElmer Informatics).

***N*-(2-((*cis*-7-Amino-8-(3,4-dichlorobenzyl)-5,6,7,8-tetrahydronaphthalen-2-yl)oxy)ethyl)propane-1-sulfonamide hydrochloride (9).** Step 1. To a solution of 7-methoxy-3,4-dihydronaphthalen-2(1*H*)-one (15 g, 85 mmol) in 200 mL of dry MeOH under nitrogen was added dropwise pyrrolidine (6.7 g, 94 mmol). The mixture was stirred for 1 h. Then the solvent was reduced under vacuum and the residue was dissolved in MeCN. At 5°C 4-(bromomethyl)-1,2-dichlorobenzene (22.5 g, 94.0 mmol) dissolved in MeCN was added and the

mixture was stirred overnight at RT. The solvent was reduced under vacuo and the residue was mixed with MeOH/DCM/H_2O 1:1:1 (50 mL, 50 mL, 50 mL) after which 10 mL of glacial acid was added. The mixture was stirred overnight. The reaction mixture was poured into a mixture of ice and H_2O and extracted 3x with DCM. The combined organic layers were washed 1x with $NaHCO_3$ solution and 1x with saturated NaCl solution. The organic phase was dried over $MgSO_4$ and the solvent was evaporated. The residue (31.5 g) was purified by flash-chromatography on silica gel with heptane/EtOAc 2:1, resulting in desired 1-(3,4-dichlorobenzyl)-7-methoxy-3,4-dihydronaphthalen-2(1*H*)-one (24.1 g, 71.7 mmol, 84%). LC−MS (ESI, *m/z*) 335.0 $[M + H]^+$, 337.0, 339.9

Step 2. To a solution of 1-(3,4-dichlorobenzyl)-7-methoxy-3,4-dihydronaphthalen-2(1*H*)-one (5.20 g, 15.5 mmol) in MeOH was added ammonium acetate (12.0 g, 155 mmol) and sodium cyanoborohydride (1.46 g, 23.3 mmol) under nitrogen. The mixture was stirred for 4 d at RT. The solvent was reduced under vacuo and extracted with EtOAc after addition of H_2O. The organic layer was washed with NaCl, dried over $MgSO_4$ and the solvent was removed. The residue was dissolved in *i*PrOH and HCl in *i*PrOH (6N) was added. After crystallization overnight the HCl-salt was separated from the mother liquor and converted to the free base with NaOH (1N). An oil was obtained which afforded *cis*-1-(3,4-dichlorobenzyl)-7-methoxy-1,2,3,4-tetrahydro-naphthalen-2-amine hydrochloride (1.9 g, 5.8 mmol, 37%) after treatment with HCl and crystallization. LC−MS (ESI, *m/z*) 336.2 $[M + H]^+$, 338.2, 340.2

Step 3. To a solution of *cis*-1-(3,4-dichlorobenzyl)-7-methoxy-1,2,3,4-tetrahydronaphthalen-2-amine hydrochloride (1.9 g, 5.8 mmol) in pyridine (10 mL) was added slowly ethyl chloroformate (1.0 g, 9.3 mmol) under nitrogen. The mixture was stirred overnight at RT, then the solvent was reduced and extracted with DCM. The organic layer was washed subsequently with HCl (1N), saturated $NaHCO_3$ solution, brine and dried over $MgSO_4$. The mixture was

filtered and concentrated affording ethyl (*cis*-1-(3,4-dichlorobenzyl)-7-methoxy-1,2,3,4-tetrahydronaphthalen-2-yl)carbamate as an orange oil that crystallized after a few hours (2.1 g, 5.1 mmol, 89%). LC−MS (ESI, *m/z*) 408.1 $[M + H]^+$, 410.1, 412.1.

Step 4. To a solution of ethyl (*cis*-1-(3,4-dichlorobenzyl)-7-methoxy-1,2,3,4-tetrahydronaphthalen-2-yl)carbamate (2.1 g, 5.1 mmol) in DCM (50 mL) was added BBr_3 (3.87 g, 15.4 mmol) at -10°C after which the reaction was allowed to warm up to RT and stirred for 2 h. A mixture of ice and H_2O was added to the mixture which was extracted with DCM. The organic layer was washed subsequently with saturated $NaHCO_3$ solution, brine, and dried over $MgSO_4$. Then the mixture was filtered and concentrated affording ethyl (*cis*-1-(3,4-dichlorobenzyl)-7-hydroxy-1,2,3,4-tetrahydronaphthalen-2-yl)carbamate as a brown oil. LC−MS (ESI, *m/z*) 394.1 $[M + H]^+$, 396.1, 398.1.

Step 5. To a suspension of NaH (55% in paraffin, 34.5 mmol) in dimethylacetatamide (80 mL) was added ethyl (*cis*-1-(3,4-dichlorobenzyl)-7-hydroxy-1,2,3,4-tetrahydronaphthalen-2-yl)carbamate (6.80 g, 17.3 mmol) dissolved in dimethylacetatamide (40 mL) and the mixture stirred for 1 h at RT. Then *tert*-butyl (2-bromoethyl)carbamate (11.6 g, 51.7 mmol) was added in portions and the mixture was stirred for further 3 d at RT. Brine was added to the reaction mixture which was extracted with EtOAc. The organic layer was washed subsequently with H_2O, brine, and dried over $MgSO_4$. Then the mixture was filtered, concentrated and the residue was purified on silica gel (flash chromatography DCM/MeOH 98:2) affording ethyl (*cis*-7-(2-((*tert*-butoxycarbonyl)amino)ethoxy)-1-(3,4-dichlorobenzyl)-1,2,3,4-tetrahydronaphthalen-2-yl)carbamate as an yellow oil (9.27 g, 17.2 mmol) which crystallized after a few hours. LC−MS (ESI, *m/z*) 481.1 $[M\text{-}t\text{-}Bu + H]^+$, 483.1, 485.1, 559.2 $[M + Na]^+$, 561.2, 563.2.

Step 6. To a solution of ethyl (*cis*-7-(2-((*tert*-butoxycarbonyl)amino)ethoxy)-1-(3,4-dichlorobenzyl)-1,2,3,4-tetrahydronaphthalen-2-yl)carbamate (9.27 g, 17.2 mmol) in DCM (200

mL) was added HCl (6M in *i*PrOH). The reaction was stirred at RT overnight. Diethyl ether was added and ethyl (*cis*-7-(2-aminoethoxy)-1-(3,4-dichlorobenzyl)-1,2,3,4-tetrahydronaphthalen-2-yl)carbamate hydrochloride precipitated out and was isolated by filtration (5.85 g, 12.3 mmol). LC−MS (ESI, *m/z*) 437.1 $[M + H]^+$, 439.1, 441.1

Step 7. To a solution of ethyl (*cis*-7-(2-aminoethoxy)-1-(3,4-dichlorobenzyl)-1,2,3,4-tetrahydronaphthalen-2-yl)carbamate hydrochloride (635 mg, 1.34 mmol) and DMAP (327 mg, 2.68 mmol) in DCM (15 mL) was added *n*-propane-1-sulfonyl chloride (191 mg, 1.34 mmol) dissolved in DCM (15 mL). The reaction mixture was stirred overnight at RT. The mixture was partitioned with H_2O, the organic fraction was collected, and the aqueous fraction was washed with DCM. The organic fractions were combined, washed subsequently with HCl (1M), saturated $NaHCO_3$ and brine, dried over $MgSO_4$, concentrated and triturated with EtOAc/diisopropylether. The mixture was filtered to obtain ethyl (*cis*-1-(3,4-dichlorobenzyl)-7-(2-(propylsulfonamido)ethoxy)-1,2,3,4-tetrahydronaphthalen-2-yl)carbamate as a white solid (600 mg, 1.10 mmol). LC−MS (ESI, *m/z*) 543.2 $[M + H]^+$, 545.2, 547.2

Step 8. A solution of ethyl (*cis*-1-(3,4-dichlorobenzyl)-7-(2-(propylsulfonamido)ethoxy)-1,2,3,4-tetrahydronaphthalen-2-yl)carbamate (600 mg, 1.10 mmol) in 30 mL KOH (20% in EtOH) was refluxed for 2 h. The mixture was partitioned with half concentrated brine/H_2O solution, the organic fraction was collected, and the aqueous fraction was washed with EtOAc. The organic fractions were combined, washed with brine, dried over $MgSO_4$, concentrated, triturated with EtOAc and filtered affording *N*-(2-((*cis*-7-amino-8-(3,4-dichlorobenzyl)-5,6,7,8-tetrahydronaphthalen-2-yl)oxy)ethyl)propane-1-sulfonamide (125 mg, 0.270 mmol). The solvent was concentrated, the obtained residue dissolved in MeOH and treated with 1M HCl. Then the MeOH was evaporated and the obtained solid was filtered and dried affording *N*-(2-((*cis*-7-amino-8-(3,4-dichlorobenzyl)-5,6,7,8-tetrahydronaphthalen-2-yl)oxy)ethyl)propane-1-

sulfonamide hydrochloride (325 mg, 0.639 mmol). LC−MS (ESI, *m/z*) 471.1 $[M + H]^+$, 473.1, 475.1, ^{1}H NMR (400 MHz, DMSO-d_6) δ (ppm) 8.32 (s, 3H), 7.55 (d, J = 8.3 Hz, 1H), 7.43 (d, J = 2.0 Hz, 1H), 7.23 (t, J = 5.9 Hz, 1H), 7.15 – 6.99 (m, 2H), 6.74 (dd, J = 8.5, 2.6 Hz, 1H), 5.70 (d, J = 2.6 Hz, 1H), 3.73 (dt, J = 10.9, 5.7 Hz, 1H), 3.55 (dt, J = 10.6, 5.3 Hz, 2H), 3.27 – 3.06 (m, 4H), 3.00 – 2.88 (m, 3H), 2.82 (dt, J = 17.5, 8.9 Hz, 1H), 2.59 – 2.53 (m, 1H), 1.99 (s, 2H), 1.71 – 1.56 (m, 2H), 0.93 (t, J = 7.4 Hz, 3H).

***N*-(2-((*cis*-7-Amino-8-(3,4-dichlorobenzyl)-5,6,7,8-tetrahydronaphthalen-2-yl)oxy)ethyl)methanesulfonamide hydrochloride (20a).** Compound **20a** (80 mg, 80% over last two steps) was prepared according to representative example **9** from ethyl (*cis*-7-(2-aminoethoxy)-1-(3,4-dichlorobenzyl)-1,2,3,4-tetrahydronaphthalen-2-yl)carbamate (100 mg, 0.229 mmol) by using methyl sulfonyl chloride in place of *n*-propane-1-sulfonyl chloride. White solid. LC−MS (ESI, *m/z*) 443.1 $[M + H]^+$, 445.1, 447.1, ^{1}H NMR (400 MHz, DMSO-d_6) δ (ppm) δ 8.46 – 8.26 (m, 3H), 7.56 (d, J = 8.2 Hz, 1H), 7.43 (d, J = 2.0 Hz, 1H), 7.21 (t, J = 6.0 Hz, 1H), 7.09 (dd, J = 8.3, 2.0 Hz, 1H), 7.06 (d, J = 8.4 Hz, 1H), 6.75 (dd, J = 8.4, 2.6 Hz, 1H), 5.70 (d, J = 2.7 Hz, 1H), 3.80 – 3.70 (m, 1H), 3.60 – 3.51 (m, 2H), 3.27 – 3.14 (m, 3H), 3.14 – 3.07 (m, 1H), 3.00 – 2.89 (m, 1H), 2.88 (s, 3H), 2.85 – 2.76 (m, 1H), 2.60 – 2.53 (m, 1H), 2.08 – 1.92 (m, 2H).

***N*-(2-((*cis*-7-Amino-8-(3,4-dichlorobenzyl)-5,6,7,8-tetrahydronaphthalen-2-yl)oxy)ethyl)butane-1-sulfonamide hydrochloride (20b)**. Compound **20b** (78 mg, 68% over last two steps) was prepared according to representative example **9** from ethyl (*cis*-7-(2-aminoethoxy)-1-(3,4-dichlorobenzyl)-1,2,3,4-tetrahydronaphthalen-2-yl)carbamate (100 mg, 0.229 mmol) by using *n*-butyl-1-sulfonyl chloride in place of *n*-propane-1-sulfonyl chloride. White solid. LC−MS (ESI, *m/z*) 485.1 $[M + H]^+$, 487.1, 489.1, ^{1}H NMR (400 MHz, DMSO-d_6) δ (ppm) 8.27 (s, 3H), 7.55 (d, J = 8.3 Hz, 1H), 7.42 (d, J = 2.0 Hz, 1H), 7.22 (t, J = 5.9 Hz, 1H),

7.12 – 7.03 (m, 2H), 6.74 (dd, J = 8.4, 2.7 Hz, 1H), 5.71 (d, J = 2.7 Hz, 1H), 3.78 – 3.70 (m, 1H), 3.60 – 3.51 (m, 2H), 3.25 – 3.12 (m, 2H), 3.12 – 3.05 (m, 1H), 3.01 – 2.89 (m, 3H), 2.87 – 2.75 (m, 1H), 2.59 – 2.54 (m, 1H), 1.99 (q, J = 9.4, 8.8 Hz, 2H), 1.64 – 1.53 (m, 2H), 1.34 (h, J = 7.4 Hz, 2H), 0.85 (t, J = 7.3 Hz, 3H).

***N*-(2-((*cis*-7-amino-8-(3,4-dichlorobenzyl)-5,6,7,8-tetrahydronaphthalen-2-yl)oxy)ethyl)-1-cyclopropylmethanesulfonamide hydrochloride (20c)**. Compound **20c** (62 mg, 56% over last two steps) was prepared according to representative example **9** from ethyl (*cis*-7-(2-aminoethoxy)-1-(3,4-dichlorobenzyl)-1,2,3,4-tetrahydronaphthalen-2-yl)carbamate (100 mg, 0.229 mmol) by using cyclopropylmethanesulfonyl chloride in place of *n*-propane-1-sulfonyl chloride. White solid. LC−MS (ESI, *m/z*) 483.1 $[M + H]^+$, 485.1, 487.1, ^{1}H NMR (400 MHz, DMSO-d_6) δ (ppm) 8.33 (s, 3H), 7.56 (d, J = 8.2 Hz, 1H), 7.42 (d, J = 2.0 Hz, 1H), 7.26 (t, J = 5.9 Hz, 1H), 7.09 (dd, J = 8.3, 2.0 Hz, 1H), 7.06 (d, J = 8.4 Hz, 1H), 6.75 (dd, J = 8.4, 2.7 Hz, 1H), 5.71 (d, J = 2.7 Hz, 1H), 3.80 – 3.70 (m, 1H), 3.64 – 3.49 (m, 2H), 3.27 – 3.14 (m, 3H), 3.14 – 3.03 (m, 1H), 3.01 – 2.89 (m, 1H), 2.88 – 2.75 (m, 1H), 2.60 – 2.54 (m, 1H), 2.10 – 1.92 (m, 2H), 0.96 – 0.83 (m, 4H).

***N*-(2-((*cis*-7-Amino-8-(3,4-dichlorobenzyl)-5,6,7,8-tetrahydronaphthalen-2-yl)oxy)ethyl)cyclobutanesulfonamide hydrochloride (20d)**. Compound **20d** (38 mg, 49% over last two steps) was prepared according to representative example **9** from ethyl (*cis*-7-(2-aminoethoxy)-1-(3,4-dichlorobenzyl)-1,2,3,4-tetrahydronaphthalen-2-yl)carbamate (70 mg, 0.16 mmol) by using cyclobutanesulfonyl chloride in place of *n*-propane-1-sulfonyl chloride. White solid. LC−MS (ESI, *m/z*) 483.1 $[M + H]^+$, 485.1, 487.1, ^{1}H NMR (500 MHz, DMSO-d_6) δ (ppm) 8.67 (s, 3H), 7.52 (d, J = 8.2 Hz, 1H), 7.46 (d, J = 2.0 Hz, 1H), 7.19 (t, J = 5.9 Hz, 1H), 7.15 – 7.00 (m, 2H), 6.73 (dd, J = 8.3, 2.7 Hz, 1H), 5.64 (d, J = 2.7 Hz, 1H), 3.89 – 3.79 (m, 1H),

3.75 – 3.65 (m, 1H), 3.57 – 3.46 (m, 2H), 3.33 – 3.27 (m, 1H), 3.25 – 3.08 (m, 3H), 2.99 – 2.88 (m, 1H), 2.88 – 2.75 (m, 1H), 2.55 – 2.44 (m, 2H), 2.29 – 2.20 (m, 2H), 2.20 – 2.09 (m, 2H), 2.09 – 1.95 (m, 2H), 1.95 – 1.78 (m, 2H).

***N*-(2-((*cis*-7-Amino-8-(3,4-dichlorobenzyl)-5,6,7,8-tetrahydronaphthalen-2-yl)oxy)ethyl)-1-methyl-1*H*-pyrazole-4-sulfonamide hydrochloride (20e)**. Compound **20e** (42 mg, 56% over last two steps) was prepared according to representative example **9** from ethyl (*cis*-7-(2-aminoethoxy)-1-(3,4-dichlorobenzyl)-1,2,3,4-tetrahydronaphthalen-2-yl)carbamate (70 mg, 0.16 mmol) by using 1-methyl-1*H*-pyrazole-4-sulfonyl chloride in place of *n*-propane-1-sulfonyl chloride. White solid. LC−MS (ESI, *m/z*) 509.1 $[M + H]^+$, 511.1, 513.1, ^{1}H NMR (400 MHz, DMSO-d_6) δ (ppm) 8.28 (s, 3H), 8.21 (s, 1H), 7.70 (s, 1H), 7.59 (t, J = 5.9 Hz, 1H), 7.54 (d, J = 8.3 Hz, 1H), 7.41 (d, J = 1.9 Hz, 1H), 7.08 (dd, J = 8.2, 2.0 Hz, 1H), 7.04 (d, J = 8.5 Hz, 1H), 6.70 (dd, J = 8.5, 2.6 Hz, 1H), 5.68 (d, J = 2.6 Hz, 1H), 3.86 (s, 3H), 3.77 – 3.68 (m, 1H), 3.62 – 3.50 (m, 2H), 3.25 – 3.16 (m, 1H), 3.13 – 3.04 (m, 1H), 3.01 – 2.88 (m, 3H), 2.86 – 2.76 (m, 1H), 2.60 – 2.53 (m, 1H), 2.05 – 1.92 (m, 2H).

***N*-(2-((*cis*-7-Amino-8-(3,4-dichlorobenzyl)-5,6,7,8-tetrahydronaphthalen-2-yl)oxy)ethyl)-1-methyl-1*H*-imidazole-4-sulfonamide hydrochloride (20f)**. Compound **20f** (34 mg, 27% over last two steps) was prepared according to representative example **9** from ethyl (*cis*-7-(2-aminoethoxy)-1-(3,4-dichlorobenzyl)-1,2,3,4-tetrahydronaphthalen-2-yl)carbamate (100 mg, 0.229 mmol) by using 1-methyl-1*H*-imidazole-4-sulfonyl chloride in place of *n*-propane-1-sulfonyl chloride. White solid. LC−MS (ESI, *m/z*) 509.1 $[M + H]^+$, 511.1, 513.1, ^{1}H NMR (400 MHz, DMSO-d_6) δ (ppm) δ 8.40 (s, 3H), 7.78 (s, 1H), 7.71 (s, 1H), 7.61 – 7.56 (m, 1H), 7.54 (d, J = 8.3 Hz, 1H), 7.42 (d, J = 1.9 Hz, 1H), 7.09 (dd, J = 8.2, 1.9 Hz, 1H), 7.04 (d, J = 8.4 Hz, 1H), 6.69 (dd, J = 8.5, 2.5 Hz, 1H), 5.68 (d, J = 2.5

Hz, 1H), 3.76 – 3.70 (m, 1H), 3.69 (s, 3H), 3.61 – 3.50 (m, 2H), 3.26 – 3.19 (m, 1H), 3.14 – 3.06 (m, 1H), 3.06 – 2.99 (m, 2H), 2.98 – 2.87 (m, 1H), 2.87 – 2.75 (m, 1H), 2.58 – 2.53 (m, 1H), 2.06 – 1.93 (m, 2H).

***N*-(2-((*cis*-7-Amino-8-(3,4-dichlorobenzyl)-5,6,7,8-tetrahydronaphthalen-2-yl)oxy)ethyl)thiophene-2-sulfonamide hydrochloride (20g)**. Compound **20g** (91 mg, 97% over last two steps) was prepared according to representative example **9** from ethyl (*cis*-7-(2-aminoethoxy)-1-(3,4-dichlorobenzyl)-1,2,3,4-tetrahydronaphthalen-2-yl)carbamate (100 mg, 0.229 mmol) by using thiophene-2-sulfonyl chloride in place of *n*-propane-1-sulfonyl chloride. White solid. LC−MS (ESI, *m/z*) 511.1 $[M + H]^+$, 513.1, 515.1, ^{1}H NMR (400 MHz, DMSO-d_6) δ (ppm) 8.36 (s, 3H), 8.06 (t, J = 5.8 Hz, 1H), 7.92 (dd, J = 4.9, 1.4 Hz, 1H), 7.58 (dd, J = 3.7, 1.4 Hz, 1H), 7.54 (d, J = 8.2 Hz, 1H), 7.42 (d, J = 1.9 Hz, 1H), 7.17 (dd, J = 5.0, 3.7 Hz, 1H), 7.08 (dd, J = 8.3, 2.0 Hz, 1H), 7.04 (d, J = 8.4 Hz, 1H), 6.69 (dd, J = 8.4, 2.6 Hz, 1H), 5.65 (d, J = 2.6 Hz, 1H), 3.76 – 3.68 (m, 1H), 3.59 – 3.50 (m, 2H), 3.25 – 3.17 (m, 1H), 3.13 – 3.01 (m, 3H), 2.99 – 2.89 (m, 1H), 2.87 – 2.74 (m, 1H), 2.58 – 2.52 (m, 1H), 2.05 – 1.94 (m, 2H).

***N*-(2-((*cis*-7-Amino-8-(3,4-dichlorobenzyl)-5,6,7,8-tetrahydronaphthalen-2-yl)oxy)ethyl)benzenesulfonamide hydrochloride (20h)**. Compound **20h** (93 mg, 91% over last two steps) was prepared according to representative example **9** from ethyl (*cis*-7-(2-aminoethoxy)-1-(3,4-dichlorobenzyl)-1,2,3,4-tetrahydronaphthalen-2-yl)carbamate (100 mg, 0.229 mmol) by using benzenesulfonyl chloride in place of *n*-propane-1-sulfonyl chloride. White solid. LC−MS (ESI, *m/z*) 505.1 $[M + H]^+$, 507.1, 509.1, ^{1}H NMR (400 MHz, DMSO-d_6) δ (ppm) 8.36 (s, 3H), 7.87 (t, J = 5.8 Hz, 1H), 7.81 – 7.76 (m, 2H), 7.67 – 7.61 (m, 1H), 7.61 – 7.55 (m, 2H), 7.52 (d, J = 8.1 Hz, 1H), 7.41 (d, J = 2.0 Hz, 1H), 7.07 (dd, J = 8.3, 2.0 Hz, 1H), 7.02 (d, J = 8.5 Hz, 1H), 6.65 (dd, J = 8.5, 2.6 Hz, 1H), 5.60 (d, J = 2.6 Hz, 1H), 3.72 – 3.63 (m, 1H), 3.58 –

3.47 (m, 2H), 3.24 – 3.17 (m, 1H), 3.13 – 3.05 (m, 1H), 3.00 – 2.88 (m, 3H), 2.86 – 2.75 (m, 1H), 2.57 – 2.53 (m, 1H), 2.05 – 1.93 (m, 2H).

***N*-(2-((*cis*-7-Amino-8-(3-chlorobenzyl)-5,6,7,8-tetrahydronaphthalen-2-yl)oxy)ethyl)-1-methyl-1*H*-imidazole-4-sulfonamide hydrochloride (20i)**. Compound **20i** (34 mg, 28% for two steps from ethyl (*cis*-7-(2-aminoethoxy)-1-(3-chlorobenzyl)-1,2,3,4-tetrahydronaphthalen-2-yl)carbamate 100 mg, 0.248 mmol) was prepared according to representative example **9** from 7-methoxy-3,4-dihydronaphthalen-2(1*H*)-one by using 1-(bromomethyl)-3-chlorobenzene in place of 4-(bromomethyl)-1,2-dichlorobenzene and 1-methyl-1*H*-imidazole-4-sulfonyl chloride in place of *n*-propane-1-sulfonyl chloride. White solid. LC−MS (ESI, *m/z*) 475.1 $[M + H]^+$, 477.1, ^{1}H NMR (500 MHz, DMSO-d_6) δ (ppm) 8.63 (s, 3H), 7.89 (s, 1H), 7.75 (s, 1H), 7.66 (s, 1H), 7.30 – 7.22 (m, 3H), 7.02 (t, J = 8.0 Hz, 2H), 6.65 (dd, J = 8.5, 2.6 Hz, 1H), 5.54 (d, J = 2.7 Hz, 1H), 3.70 (s, 3H), 3.64 (dt, J = 9.9, 6.0 Hz, 1H), 3.58 – 3.50 (m, 1H), 3.47 (dt, J = 10.0, 6.1 Hz, 1H), 3.31 – 3.25 (m, 1H), 3.22 – 3.17 (m, 1H), 3.05 – 2.98 (m, 2H), 2.97 – 2.90 (m, 1H), 2.86 – 2.75 (m, 1H), 2.49 – 2.41 (m, 1H), 2.08 – 1.96 (m, 2H).

***N*-(2-((*cis*-7-Amino-8-(4-chlorobenzyl)-5,6,7,8-tetrahydronaphthalen-2-yl)oxy)ethyl)-1-methyl-1*H*-imidazole-4-sulfonamide hydrochloride (20j)**. Compound **20j** (50 mg, 22% for two steps from ethyl (*cis*-7-(2-aminoethoxy)-1-(4-chlorobenzyl)-1,2,3,4-tetrahydronaphthalen-2-yl)carbamate 150 mg, 0.372 mmol) was prepared according to representative example **9** from 7-methoxy-3,4-dihydronaphthalen-2(1*H*)-one by using 1-(bromomethyl)-4-chlorobenzene in place of 4-(bromomethyl)-1,2-dichlorobenzene and 1-methyl-1*H*-imidazole-4-sulfonyl chloride in place of *n*-propane-1-sulfonyl chloride. White solid. LC−MS (ESI, *m/z*) 475.1 $[M + H]^+$, 477.1, ^{1}H NMR (500 MHz, DMSO-d_6) δ (ppm) 8.72 (s, 3H), 7.92 (s, 1H), 7.75 (s, 1H), 7.68 (s, 1H), 7.30 (d, J = 8.0 Hz, 2H), 7.14 (d, J = 8.1 Hz, 2H), 7.00 (d, J = 8.5

Hz, 1H), 6.64 (dd, J = 8.3, 2.6 Hz, 1H), 5.54 (d, J = 2.6 Hz, 1H), 3.70 (s, 3H), 3.68 – 3.63 (m, 1H), 3.55 – 3.44 (m, 2H), 3.33 – 3.26 (m, 1H), 3.20 (dd, J = 13.2, 3.2 Hz, 1H), 3.06 – 2.97 (m, 2H), 2.96 – 2.88 (m, 1H), 2.84 – 2.74 (m, 1H), 2.43 (t, J = 12.1 Hz, 1H), 2.09 – 1.95 (m, 2H).

***N*-(2-((*cis*-7-Amino-8-benzyl-5,6,7,8-tetrahydronaphthalen-2-yl)oxy)ethyl)-1-methyl-1*H*-imidazole-4-sulfonamide hydrochloride (20k)**. Compound **20k** (480 mg, 93% last step from ethyl (*cis*-1-benzyl-7-(2-((1-methyl-1*H*-imidazole)-4-sulfonamido)ethoxy)-1,2,3,4-tetrahydronaphthalen-2-yl)carbamate 600 mg, 1.17 mmol) was prepared according to representative example **9** from 7-methoxy-3,4-dihydronaphthalen-2(1*H*)-one by using (bromomethyl)benzene in place of 4-(bromomethyl)-1,2-dichlorobenzene and 1-methyl-1*H*-imidazole-4-sulfonyl chloride in place of *n*-propane-1-sulfonyl chloride. White solid. LC−MS (ESI, *m/z*) 441.1 $[M + H]^+$, ^{1}H NMR (500 MHz, DMSO-d_6) δ (ppm) 8.74 (s, 3H), 8.08 (s, 1H), 7.81 (s, 1H), 7.78 (s, 1H), 7.24 (t, J = 7.4 Hz, 2H), 7.17 (t, J = 7.3 Hz, 1H), 7.10 (d, J = 7.3 Hz, 2H), 6.98 (d, J = 8.5 Hz, 1H), 6.60 (dd, J = 8.4, 2.6 Hz, 1H), 5.46 (d, J = 2.7 Hz, 1H), 3.71 (s, 3H), 3.56 (dt, J = 9.9, 5.9 Hz, 1H), 3.53 – 3.46 (m, 1H), 3.36 (dt, J = 9.9, 6.0 Hz, 1H), 3.33 – 3.28 (m, 1H), 3.23 (dd, J = 13.1, 3.2 Hz, 1H), 3.03 – 2.96 (m, 2H), 2.96 – 2.88 (m, 1H), 2.79 (dt, J = 17.7, 9.1 Hz, 1H), 2.38 (t, J = 12.1 Hz, 1H), 2.10 – 1.97 (m, 2H).

***N*-(2-((*cis*-7-Amino-8-(2-chlorobenzyl)-5,6,7,8-tetrahydronaphthalen-2-yl)oxy)ethyl)-1-methyl-1*H*-imidazole-4-sulfonamide hydrochloride (20l)**. Compound **20l** (9 mg, 8% for last step from ethyl (*cis*-1-(2-chlorobenzyl)-7-(2-((1-methyl-1*H*-imidazole)-4-sulfonamido)ethoxy)-1,2,3,4-tetrahydronaphthalen-2-yl)carbamate 100 mg, 0.183 mmol) was prepared according to representative example **9** from 7-methoxy-3,4-dihydronaphthalen-2(1*H*)-one by using 1-(bromomethyl)-2-chlorobenzene in place of 4-(bromomethyl)-1,2-dichlorobenzene and 1-methyl-1*H*-imidazole-4-sulfonyl chloride in place of

n-propane-1-sulfonyl chloride. White solid. LC−MS (ESI, *m/z*) 475.1 $[M + H]^+$, 477.1. ^{1}H NMR (500 MHz, DMSO-d_6) δ (ppm) 8.34 (s, 3H), 7.77 (d, J = 1.3 Hz, 1H), 7.71 (d, J = 1.4 Hz, 1H), 7.55 (t, J = 5.9 Hz, 1H), 7.34 (dd, J = 7.1, 2.0 Hz, 1H), 7.28 – 7.21 (m, 2H), 7.21 – 7.16 (m, 1H), 7.00 (d, J = 8.5 Hz, 1H), 6.64 (dd, J = 8.4, 2.6 Hz, 1H), 5.44 (d, J = 2.6 Hz, 1H), 3.69 (s, 3H), 3.64 – 3.54 (m, 3H), 3.25 (d, J = 11.4 Hz, 1H), 3.11 (dd, J = 13.1, 3.8 Hz, 1H), 3.02 – 2.93 (m, 3H), 2.88 – 2.75 (m, 2H), 2.15 – 1.97 (m, 2H).

***N*-(2-((*cis*-7-Amino-8-(3-chloro-5-fluorobenzyl)-5,6,7,8-tetrahydronaphthalen-2-yl)oxy)ethyl)-1-methyl-1*H*-imidazole-4-sulfonamide hydrochloride (20m)**. Compound **20m (**81 mg, 73% for last step from ethyl (*cis*-1-(3-chloro-5-fluorobenzyl)-7-(2-((1-methyl-1*H*-imidazole)-4-sulfonamido)ethoxy)-1,2,3,4-tetrahydronaphthalen-2-yl)carbamate 118 mg, 0.209 mmol) was prepared according to representative example **9** from 7-methoxy-3,4-dihydronaphthalen-2(1*H*)-one by using 1-(bromomethyl)-3-chloro-5-fluorobenzene in place of 4-(bromomethyl)-1,2-dichlorobenzene and 1-methyl-1*H*-imidazole-4-sulfonyl chloride in place of *n*-propane-1-sulfonyl chloride. White solid. LC−MS (ESI, *m/z*) 493.1 $[M + H]^+$, 495.1, ^{1}H NMR (400 MHz, DMSO-d_6) δ (ppm) 8.41 (s, 3H), 7.78 (d, J = 1.4 Hz, 1H), 7.70 (d, J = 1.4 Hz, 1H), 7.63 – 7.52 (m, 1H), 7.29 – 7.22 (m, 1H), 7.10 – 6.99 (m, 3H), 6.70 (dd, J = 8.5, 2.7 Hz, 1H), 5.70 (d, J = 2.7 Hz, 1H), 3.69 (s, 3H), 3.56 (dt, J = 9.8, 6.1 Hz, 2H), 3.27 (dt, J = 10.7, 3.9 Hz, 1H), 3.13 (dd, J = 13.4, 3.6 Hz, 1H), 3.09 – 3.01 (m, 2H), 2.93 (dt, J = 17.2, 5.0 Hz, 1H), 2.81 (dt, J = 17.5, 8.9 Hz, 1H), 2.62 – 2.53 (m, 1H), 2.06 – 1.94 (m, 2H).

***N*-(2-((*cis*-7-Amino-8-(3-(trifluoromethyl)benzyl)-5,6,7,8-tetrahydronaphthalen-2-yl)oxy)ethyl)-1-methyl-1*H*-imidazole-4-sulfonamide hydrochloride (20n)**. Compound **20m** (102 mg, 54% for last step from ethyl (*cis*-7-(2-((1-

methyl-1*H*-imidazole)-4-sulfonamido)ethoxy)-1-(3-(trifluoromethyl)benzyl)-1,2,3,4-tetrahydronaphthalen-2-yl)carbamate 180 mg, 0.310 mmol) was prepared according to representative example **9** from 7-methoxy-3,4-dihydronaphthalen-2(1*H*)-one by using 1-(bromomethyl)-3-(trifluoromethyl)benzene in place of 4-(bromomethyl)-1,2-dichlorobenzene and 1-methyl-1*H*-imidazole-4-sulfonyl chloride in place of *n*-propane-1-sulfonyl chloride. White solid. LC−MS (ESI, *m/z*) 509.2 $[M + H]^+$, ^{1}H NMR (400 MHz, DMSO-d_6) δ (ppm) 8.39 (s, 3H), 8.19 (s, 1H), 7.69 (s, 1H), 7.59 – 7.47 (m, 3H), 7.41 (s, 1H), 7.37 (d, J = 7.6 Hz, 1H), 7.03 (d, J = 8.4 Hz, 1H), 6.66 (dd, J = 8.4, 2.5 Hz, 1H), 5.46 (d, J = 2.9 Hz, 1H), 3.86 (s, 3H), 3.63 – 3.52 (m, 2H), 3.40 (dt, J = 10.6, 5.9 Hz, 1H), 3.27 – 3.16 (m, 2H), 3.00 – 2.88 (m, 3H), 2.82 (dt, J = 17.6, 9.0 Hz, 1H), 2.61 (t, J = 11.8 Hz, 1H), 2.12 – 1.94 (m, 2H).

***N*-(2-(((7*S*,8*R*)-7-(Azetidin-1-yl)-8-benzyl-5,6,7,8-tetrahydronaphthalen-2-yl)oxy)ethyl)-1-methyl-1*H*-imidazole-4-sulfonamide ((7*S*,8*R*)-27a)**. Step 1. In a three-necked flask equipped with a Dean-Stark apparatus, heating mantle and magnetic stirrer were charged 1-benzyl-7-methoxy-3,4-dihydronaphthalen-2(1*H*)-one (120 g, 451 mmol), propionamide (82.00 g, 1126 mmol) and *p*-toluenesulfonic acid monohydrate (17 g, 90 mmol) followed by toluene (1.8 L). The resulting solution was heated to reflux for 5 days and monitored by HPLC (about 16% of starting material remained). The reaction mixture was cooled to RT and washed with 8% aqueous sodium bicarbonate solution (250 mL) and H_2O (250 mL). The layers were separated. The organic layer was concentrated to near dryness and chase distilled with isopropylalcohol (100 mL). The crude product was transferred to a flask equipped with a mechanical stirrer, heating mantle and nitrogen inlet. Isopropylalcohol (500 mL) was added to the flask and the suspension was heated to 62°C and all the solids were dissolved. The suspension was allowed to cool over 2 h to 30°C then cooled to 5°C. Solids were filtered and washed with mixture of heptane/ isopropylalcohol (4:1, 100 mL). Solids were dried under vacuum to give 93.5

g (yield: 65%) *N*-(1-benzyl-7-methoxy-3,4-dihydronaphthalen-2-yl)propionamide (**21**) as a white solid. LC−MS (ESI, *m/z*) 322.2 $[M+H]^+$, ^{1}H NMR (400 MHz, Chloroform-*d*) δ (ppm) 7.31 – 7.25 (m, 2H), 7.23 – 7.16 (m, 3H), 7.05 (d, J = 8.1 Hz, 1H), 6.72 (d, J = 2.5 Hz, 1H), 6.66 (s, 1H), 6.64 (dd, J = 8.1, 2.5 Hz, 1H), 3.83 (s, 2H), 3.68 (s, 3H), 2.87 – 2.74 (m, 4H), 2.19 (q, J = 7.6 Hz, 2H), 1.09 (t, J = 7.5 Hz, 3H).

Step 2. Chlorocyclooctadiene rhodium(I) dimer (0.019 g, 0.039 mmol, 0.078 mmol of Rh), Josiphos (SLJ216-2, 0.050 g, 0.078 mmol), and *N*-(l-benzyl-7-methoxy-3,4-dihydronaphthalen-2-yl)propionamide (10.0 g, 31.1 mmol) were combined in a metal reactor, and the vessel was inerted with argon. Degassed MeOH (100 mL) was added by cannula, then the mixture was agitated under argon at 50°C for 20 min. The vessel was pressurized with 60 psig of hydrogen and agitated at 55°C for 25 h. HPLC analysis indicated complete conversion and 95.9% ee. The MeOH solution of the crude reduction product was concentrated and triturated with heptane to yield desired *N*-((1*R*,2*S*)-1-benzyl-7-methoxy-1,2,3,4-tetrahydronaphthalen-2-yl)propionamide **((1*R*,2*S*)-22**, 9.7 g, 30 mmol, 96.6% purity, 93% yield, 95.8% ee). LC−MS (ESI, m/z) 324.1 $[M+H]^+$, ^{1}H NMR (400 MHz, DMSO-d6) δ (ppm) 7.27 (2H, m), 7.20 (1H, m), 7.12 (2H, m), 7.00 (1H, d), 6.70 (1H, d), 6.36 (1H, d), 5.32 (NH, d), 4.31 (1H, m), 3.59 (3H, s), 3.38 (1H, m), 2.90 (4H, m), 2.01 (3H, m), 1.86 (1H, m), 1.06, (3H, t). ^{1}H NMR (400 MHz, Chloroform-d) δ (ppm) 7.30 – 7.25 (m, 2H), 7.22 – 7.17 (m, 1H), 7.15 – 7.10 (m, 2H), 7.00 (d, J = 8.4 Hz, 1H), 6.69 (dd, J = 8.4, 2.7 Hz, 1H), 6.34 (d, J = 2.7 Hz, 1H), 5.37 (d, J = 8.1 Hz, 1H), 4.35 – 4.26 (m, 1H), 3.58 (s, 3H), 3.41 – 3.33 (m, 1H), 2.96 – 2.82 (m, 4H), 2.08 – 1.92 (m, 3H), 1.89 – 1.79 (m, 1H), 1.06 (t, J = 7.6 Hz, 3H).

Step 3. *N*-((1*R*,2*S*)-1-benzyl-7-methoxy-1,2,3,4-tetrahydronaphthalen-2-yl)propionamide (98.0 g, 303 mmol) was slurried in H_2O (882 mL) and 882 mL of acetic acid at 25°C. To this suspension was added concentrated sulfuric acid (323 mL, 5.8 mol, 19.2 equiv). The mixture was

heated to reflux (108-109°C) for 68 h. The reaction mixture was allowed to cool to RT and 1.5 L of H_2O were added. The slurry was cooled to 4°C and the solid was filtered off. The solid was then slurried in 400 mL of MeCN at RT. After stirring for 30 min., the solid was cooled in an ice bath, filtered, washed with cold MeCN and dried in the vacuum oven at 45°C to yield desired (1*R*,2*S*)-1-benzyl-7-methoxy-1,2,3,4-tetrahydronaphthalen-2-amine hemisulfate ((1*R*,2*S*)-**13**) (71.4 g, 225 mmol, 75%). LC−MS (ESI, *m/z*) 268.2 $[M+H]^+$, ^{1}H NMR (400 MHz, DMSO-d_6) δ (ppm) 8.55 – 7.78 (br, s, 3H), 7.29 – 7.22 (m, 2H), 7.22 – 7.16 (m, 1H), 7.07 – 7.02 (m, 2H), 6.97 (d, J = 8.5 Hz, 1H), 6.62 (dd, J = 8.4, 2.7 Hz, 1H), 5.54 (d, J = 2.7 Hz, 1H), 3.52 (dt, J = 11.2, 4.4 Hz, 1H), 3.26 (s, 3H), 3.15 (dt, J = 10.9, 4.0 Hz, 1H), 3.08 (dd, J = 12.9, 3.4 Hz, 1H), 2.95 – 2.86 (m, 1H), 2.84 – 2.71 (m, 1H), 2.45 – 2.39 (m, 1H), 2.04 – 1.87 (m, 2H).

Step 4. A solution of (1*R,*2*S*)-1-benzyl-7-methoxy-1,2,3,4-tetrahydronaphthalen-2-amine hemisulfate ((**1*R,2S***)-**13**) (20 g, 63 mmol) in HBr (130 mL, 48%) and acetic acid (130 mL) in a 500 mL three neck flask equipped with mechanical stirrer was heated to 110°C for 1.5 h. Then the solvent was distilled off under high vacuum, the thick slurry collected in 200 mL of H_2O and cooled in a dry ice bath to 0°C. Ammonium hydroxide (28%) was added dropwise keeping temperature below 5°C until pH 8-9 range. The product was extracted 2x250 mL of DCM containing 5% MeOH. The combined organic layers were washed with of saturated sodium bicarbonate, dried over $MgSO_4$, filtered and concentrated to give off white solid. This material was triturated in 200 mL of heptane, filtered, washed with heptane 50 mL and dried affording (7*S,*8*R*)-7-amino-8-benzyl-5,6,7,8-tetrahydronaphthalen-2-ol as a white solid (14.6g, 57.6 mmol, 90%). LC−MS (ESI, *m/z*) 254.1 $[M + H]^+$.

Step 5. A 500 three neck flask equipped with mechanical stirrer, water condenser and nitrogen inlet, was charged with (7*S,*8*R*)-7-amino-8-benzyl-5,6,7,8-tetrahydronaphthalen-2-ol (10.0 g, 39.5 mmol), 1,3-dibromopropane (4.41 mL, 43.4 mmol), MeCN (100 mL) and *N*,*N*-

diisopropylethylamine (14.3 mL, 83.0 mmol). The reaction mixture was heated to 70°C under nitrogen for 19hrs then cooled to 40ºC, and stirred for 30 minutes. The suspension was filtered and the filtercake washed with 40 mL of chilled MeCN, 2x40 mL H_2O, and MeCN (25 mL), and then dried to obtain (7*S,*8*R*)-7-(azetidin-1-yl)-8-benzyl-5,6,7,8-tetrahydronaphthalen-2-ol (5.9 g, 20.1 mmol, 51%). Part of it was further converted to the desired product according to representative example (**9**) following steps 5-7 by using 1-methyl-1*H*-imidazole-4-sulfonyl chloride in place of *n*-propane-1-sulfonyl chloride (1.43 g, 2.85 mmol). $[\alpha]^{25}_{D}$ -81.4 as fumarate (*c* 0.41, MeOH). LC−MS (ESI, *m/z*) 481.2 $[M + H]^+$, ^{1}H NMR (500 MHz, DMSO-d_6) δ (ppm) 7.75 (s, 1H), 7.70 (s, 1H), 7.58 – 7.51 (m, 1H), 7.22 (t, J = 7.4 Hz, 2H), 7.15 (t, J = 7.3 Hz, 1H), 6.99 – 6.90 (m, 3H), 6.58 (dd, J = 8.5, 2.7 Hz, 1H), 5.59 (d, J = 2.7 Hz, 1H), 3.68 (s, 3H), 3.61 (dt, J = 11.5, 6.1 Hz, 1H), 3.45 (dt, J = 10.4, 6.0 Hz, 1H), 3.31 – 3.26 (m, 1H), 3.26 – 3.17 (m, 4H), 3.03 – 2.95 (m, 2H), 2.86 – 2.77 (m, 2H), 2.73 – 2.62 (m, 1H), 2.37 (dt, J = 12.4, 3.8 Hz, 1H), 2.25 – 2.16 (m, 1H), 2.03 – 1.95 (m, 2H), 1.71 – 1.64 (m, 1H), 1.57 – 1.45 (m, 1H).

***N*-(2-(((7*S*,8*R*)-8-Benzyl-7-(pyrrolidin-1-yl)-5,6,7,8-tetrahydronaphthalen-2-yl)oxy)ethyl)-1-methyl-1*H*-imidazole-4-sulfonamide maleate ((7*S*,8*R*)-27b)**. Compound **(7*S*,8*R*)-27b** (0.7 g, 99% for last step from 2-(((7*S*,8*R*)-8-benzyl-7-(pyrrolidin-1-yl)-5,6,7,8-tetrahydronaphthalen-2-yl)oxy)ethan-1-amine 0.500 g, 1.43 mmol) was prepared according to compound (**7*S*,8*R*)-27a** by using 1,3-dibromobutane in place of 1,3-dibromopropane. White solid. $[\alpha]^{25}_{D}$ -75.6 as hydrochloride (*c* 0.38, MeOH). LC−MS (ESI, *m/z*) 495.2 $[M + H]^+$, ^{1}H NMR (400 MHz, Chloroform-*d*) δ (ppm) 7.45 (d, J = 1.4 Hz, 1H), 7.42 (d, J = 1.4 Hz, 1H), 7.24 – 7.13 (m, 3H), 6.97 – 6.91 (m, 3H), 6.56 (dd, J = 8.3, 2.7 Hz, 1H), 5.51 (d, J = 2.7 Hz, 1H), 5.03 (t, J = 6.0 Hz, 1H), 3.72 (s, 3H), 3.68 – 3.61 (m, 1H), 3.46 – 3.38 (m, 2H), 3.28 – 3.20 (m, 2H), 3.06 – 2.99 (m, 1H), 2.96 – 2.88 (m, 1H), 2.83 (dd, J = 11.1, 7.3 Hz, 1H),

2.81 – 2.73 (m, 2H), 2.73 – 2.65 (m, 1H), 2.44 – 2.31 (m, 2H), 2.13 – 2.04 (m, 1H), 1.98 – 1.82 (m, 5H).

***N*-(2-(((7*S*,8*R*)-7-(Azetidin-1-yl)-8-benzyl-5,6,7,8-tetrahydronaphthalen-2-yl)oxy)ethyl)-1-cyclopropylmethanesulfonamide ((7*S*,8*R*)-27c)**. Compound **(7*S*,8*R*)-27c** (150 mg, 56% for last step from 2-(((7*S*,8*R*)-7-(azetidin-1-yl)-8-benzyl-5,6,7,8-tetrahydronaphthalen-2-yl)oxy)ethan-1-amine 0.200 g, 0.594 mmol) was prepared according to compound (**7*S*,8*R*)-27a** by using cyclopropylmethanesulfonyl chloride in place of 1-methyl-1*H*-imidazole-4-sulfonyl chloride. White solid. $[\alpha]^{25}_{D}$ -104.0 (*c* 0.42, MeOH). LC−MS (ESI, *m/z*) 455.3 $[M + H]^+$, ^{1}H NMR (500 MHz, DMSO-d_6) δ (ppm) 7.25 (t, J = 7.4 Hz, 2H), 7.23 – 7.15 (m, 2H), 7.01 – 6.92 (m, 3H), 6.64 (dd, J = 8.4, 2.7 Hz, 1H), 5.63 (d, J = 2.7 Hz, 1H), 3.63 (dt, J = 10.8, 5.7 Hz, 1H), 3.44 (dt, J = 10.3, 5.6 Hz, 1H), 3.36 – 3.29 (m, 1H), 3.27 – 3.18 (m, 3H), 3.18 – 3.13 (m, 2H), 2.94 (d, J = 7.1 Hz, 2H), 2.83 (dd, J = 16.7, 7.7 Hz, 2H), 2.76 – 2.63 (m, 1H), 2.42 – 2.35 (m, 1H), 2.26 – 2.18 (m, 1H), 2.06 – 1.96 (m, 2H), 1.74 – 1.65 (m, 1H), 1.60 – 1.47 (m, 1H), 1.03 – 0.94 (m, 1H), 0.58 – 0.51 (m, 2H), 0.33 – 0.27 (m, 2H).

***N*-(2-(((3*R*,4*R*)-3-(Azetidin-1-yl)-4-benzylchroman-6-yl)oxy)ethyl)-1-methyl-1*H*-imidazole-4-sulfonamide ((3*R*,4*R*)-36a)**. Step 1. 6-Methoxychroman-4-one (5.20 g, 29.2 mmol) was dissolved in EtOH and hydroxylamine hydrochloride (2.53 g, 36.5 mmol) and sodium acetate (2.99 g, 36.5 mmol) dissolved in 10 mL of H_2O were added. The mixture was stirred at 65°C for 1.5 h. The mixture was allowed to cool to RT and concentrated. The residue was dissolved in methyl-*tert*-butylether. The organic phase was washed with H_2O, dried over $MgSO_4$ and concentrated to give crude 6-methoxychroman-4-one oxime (5.68 g, 29.4 mmol, quant.), which was directly used in the next step. LC−MS (ESI, *m/z*) 194.1 $[M + H]^+$.

Step 2. 6-Methoxychroman-4-one oxime (5.68 g, 29.4 mmol) was dissolved under argon atmosphere in 30 mL of dry pyridine. At 0°C 4-methylbenzene-l-sulfonyl chloride (6.05 g, 31.8 mmol) of was added in small portions over 40 min. The mixture was stirred at 0°C for an additional hour and then warmed to RT and stirred overnight. The mixture was poured into a mixture of 260 mL ice and H_2O, stirred, and the suspension was filtered. The solid residue was washed with a small amount of cold H_2O (2x) and cold EtOH (lx), and dried to yield desired 6-methoxychroman-4-one *O*-tosyl oxime (8.96 g, 25.8 mmol, 88%). LC−MS (ESI, *m/z*) 348.0 $[M + H]^+$.

Step 3. To a solution of sodium ethoxide (10.5 mL, 28.1 mmol, 21% in EtOH) under nitrogen atmosphere at 0°C was added a suspension of (*Z*)-6-methoxychroman-4-one *O*-tosyl oxime (8.96 g, 25.8 mmol) in toluene. The mixture was stirred overnight and slowly warmed to RT. The suspension was filtered and rinsed with ether. An aqueous solution of HCl (95.0 mL, 190 mmol, 2M) was added to the filtrate and stirred at RT for 2 h. The suspension was diluted with 150 mL of H_2O and phases were separated. The organic phase was extracted with aqueous HCl solution (2x, 20-30 mL, 1 N) and H_2O (lx, 30 mL). The combined aqueous layers were washed with ether (lx). The aqueous phase was stirred with a small amount of activated charcoal, filtered, and concentrated to a 1/5 of its volume until a crystalline precipitation was observed. The mixture was cooled to 0° C and the crystalline material was filtered off, washed with a small amount of cold EtOH, and dried in vacuo. The filtrate was concentrated, combined with the first precipitate affording crude 3-amino-6-methoxychroman-4-one hydrochloride (3.67 g, 15.9 mmol, 62%) LC−MS (ESI, *m/z*) 194.1 $[M + H]^+$.

Step 4. 3-Amino-6-methoxychroman-4-one hydrochloride (2.82 g, 12.3 mmol) was dissolved in THF under nitrogen atmosphere and cooled to 0°C with an ice bath. Diisopropylethylamine and ethyl chloroformate were added. The mixture was allowed to warm to RT and stirred for 30

min. The mixture was diluted with EtOAc and washed with saturated ammonium chloride solution (2x) and H_2O (lx). The organic phase was washed, dried over $MgSO_4$, and concentrated to give crude ethyl (6-methoxy-4-oxochroman-3-yl)carbamate (3.50 g, 13.2 mmol, quant.) of. LC−MS (ESI, *m/z*) 266.1 $[M + H]^+$.

Step 5. Benzylmagnesium chloride (26.4 mL, 52.8 mmol) of under nitrogen atmosphere were cooled to 0°C with an ice bath and ethyl (6-methoxy-4-oxochroman-3-yl)carbamate (3.50 g, 13.2 mmol) dissolved in 100 mL dry THF was slowly added. The mixture was stirred at 0°C for 1 h. The cooling bath was removed and saturated ammonium chloride solution was added. H_2O was added until a clear solution was obtained. The phases were separated and the organic phase was washed with saturated ammonium chloride solution, dried over $MgSO_4$, and concentrated to give crude ethyl (4-benzyl-4-hydroxy-6-methoxychroman-3-yl)carbamate (6.8 g, crude). LC−MS (ESI, *m/z*) 340.1 $[M\text{-}H_2O + H]^+$, 380.1 $[M + Na]^+$.

Step 6. Ethyl (4-benzyl-4-hydroxy-6-methoxychroman-3-yl)carbamate (6.8 g, crude) was added to 80 mL of half concentrated aqueous hydrochloric acid and stirred at 100°C for 2.5 h. The mixture was cooled to 0°C and diluted with H_2O. Sodium hydroxide (50% aqueous solution) was carefully added until pH >10. The aqueous phase was extracted with EtOAc (2x). The combined organic phases were washed with H_2O and brine, dried over $MgSO_4$ and the solvent was evaporated to give 5.7 g of crude material, which was purified by flash chromatography to yield the desired product ethyl (4-benzylidene-6-methoxychroman-3 –yl)carbamate (3.1 g, 9.1 mmol, 69% over last two steps). LC−MS (ESI, *m/z*) 340.2 $[M + H]^+$.

Step 7. Ethyl (4-benzylidene-6-methoxychroman-3-yl)carbamate (3.1 g, 9.1 mmol) was dissolved in 80 mL of EtOH and Pd/C (910 mg, 0.9 mmol) was added. Then, ammonium formate (5.8 g, 91 mmol) dissolved in 20 mL of H_2O was added and the mixture was warmed to 70°C and stirred for 1.5 h. The mixture was cooled to RT. The catalyst was filtered off and washed with

EtOH/H_2O. The filtrate was concentrated in vacuo to remove EtOH. The aqueous concentrate was extracted with EtOAc (2x). The combined organic phases were dried over $MgSO_4$ and the solvent was evaporated to yield crude ethyl (4-benzyl-6-methoxychroman-3-yl)carbamate (3.2 g, 9.3 mmol, *cis*:*trans* ~ 7:1). The *cis*-isomer can be enriched (-26:1) by crystallization from hot heptane. LC−MS (ESI, *m/z*) 342.1 $[M + H]^+$.

Step 8. Ethyl (4-benzyl-6-methoxychroman-3-yl)carbamate (3.2 g, 9.3 mmol) under nitrogen atmosphere was dissolved in 90 mL of DCM. At 0°C boron tribromide (28.0 mL, 28.0 mmol, 1M in DCM) was added. The reaction mixture was stirred at 0°C for 2 h. At 0°C saturated sodium hydrogencarbonate solution was added to the reaction mixture. The phases were separated and the aqueous phase was extracted with DCM. The combined organic layers were washed with brine, dried over $MgSO_4$ and the solvent was evaporated to yield crude ethyl (4-benzyl-6-hydroxychroman-3-yl)carbamate (3.0 g, 9.2 mmol, 99%) of. LC−MS (ESI, *m/z*) 328.1 $[M + H]^+$.

Step 9. Ethyl (4-benzyl-6-hydroxychroman-3-yl)carbamate (2.3 g, 7.0 mmol) of was dissolved in ethanolic KOH 20% and stirred at 70°C overnight. The solvent was evaporated, the residue partitioned between EtOAc and H_2O. The organic layer was washed twice with H_2O and the combined H_2O layer extracted another 2 times with EtOAc. The combined EtOAc extract was dried over $MgSO_4$, filtered and evaporated. The crude 3-amino-4-benzylchroman-6-ol was purified by flash chromatography to yield pure *cis*-isomer (1,11 g, 4.34 mmol, 62%) and *trans*-isomer (0.25 g, 0.97 mmol, 14%). LC−MS *cis*-isomer (ESI, *m/z*) 256.0 $[M + H]^+$.

Step 10. *cis*-3-amino-4-benzylchroman-6-ol (0.911 g, 3.57 mmol), 1,3-dibromopropane (0.36 mL, 3.55 mmol) and *N*-ethyl-*N*-isopropylpropan-2-amine (1.90 mL, 10.8 mmol) were combined with 18 mL MeCN and stirred at 130°C in the microwave (CEM) for 3 hours. Additional 75 mL 1,3-dibromopropane and 0.5 mL N-ethyl-N-isopropylpropan-2-amine were added to the reaction mixture (brown solution) and stirred at 130°C in the microwave (CEM) for an additional 1 h. The

reaction mixture was evaporated and the obtained residue partitioned between H_2O and EtOAc. The organic phase was washed with H_2O and brine and the combined aqueous phases extracted twice with EtOAc. Combined organic extracts were dried over $MgSO_4$, filtrated and evaporated to dryness to yield 1 g of crude material. The material was purified by flash chromatography to yield pure *cis*-3-(azetidin-1-yl)-4-benzylchroman-6-ol (594 mg, 2.01 mmol, 56%) of. LC−MS (ESI, *m/z*) 296.2 $[M + H]^+$.

Step 11. Compound *cis*- *N*-(2-((3-(azetidin-1-yl)-4-benzylchroman-6-yl)oxy)ethyl)-1-methyl-1*H*-imidazole-4-sulfonamide (320 mg, 0.663 mmol) was subsequently prepared according to steps 5-7 of compound (**9**) by using 1-methyl-1*H*-imidazole-4-sulfonyl chloride in place of *n*-propane-1-sulfonyl chloride and TFA instead of HCl in *i*PrOH for the cleavage of the BOC group. LC−MS (ESI, *m/z*) 483.2 $[M + H]^+$.

Step 12. The racemate of compound **36a** (320 mg, 0.663 mmol) was separated by chiral chromatography on Chiracel AD 2 x 25 cm (*n*-heptane/EtOH 50:50, 0.1% TEA) isocratic (t_R [min] = 13.65 und 18.14). *N*-(2-(((3*R*,4*R*)-3-(azetidin-1-yl)-4-benzylchroman-6-yl)oxy)ethyl)-1-methyl-1*H*-imidazole-4-sulfonamide (t_R = 18.14 min): white solid (44 mg, 0.09 mmol). $[\alpha]^{25}_D$ -322.3 (*c* 0.273, MeOH), LC−MS (ESI, *m/z*) 483.2 $[M + H]^+$, ^{1}H NMR (500 MHz, Chloroform-*d*) δ (ppm) 7.44 (dd, J = 13.4, 1.5 Hz, 2H), 7.27 – 7.17 (m, 3H), 7.01 – 6.97 (m, 2H), 6.68 (d, J = 8.9 Hz, 1H), 6.56 (dd, J = 8.9, 3.0 Hz, 1H), 5.53 (d, J = 3.0 Hz, 1H), 5.22 (t, J = 6.3 Hz, 1H), 4.04 – 3.99 (m, 1H), 3.90 (t, J = 10.8 Hz, 1H), 3.72 (s, 3H), 3.63 (dt, J = 10.3, 5.3 Hz, 1H), 3.48 (dt, J = 9.9, 5.1 Hz, 1H), 3.45 – 3.36 (m, 4H), 3.28 (dd, J = 13.2, 3.3 Hz, 1H), 3.23 (q, J = 5.5 Hz, 2H), 2.93 – 2.88 (m, 1H), 2.85 – 2.77 (m, 1H), 2.46 – 2.38 (m, 1H), 2.19 (p, J = 6.9 Hz, 2H).

***N*-(2-((*cis*-3-(Azetidin-1-yl)-4-benzylchroman-6-yl)oxy)ethyl)-1-cyclopropylmethanesulfonamide (36b)**. Compound **36b** (17 mg, 23% for last step from

2-((*cis*-3-(azetidin-1-yl)-4-benzylchroman-6-yl)oxy)ethan-1-amine 55 mg, 0.16 mmol) was prepared according to example **36a** by using cyclopropylmethanesulfonyl chloride in place of 1-methyl-1*H*-imidazole-4-sulfonyl chloride. White solid. LC−MS (ESI, *m/z*) 457.2 $[M + H]^+$, ^1H NMR (400 MHz, Chloroform-*d*) δ (ppm) 7.29 – 7.18 (m, 3H), 7.03 – 6.98 (m, 2H), 6.71 (d, J = 8.8 Hz, 1H), 6.60 (dd, J = 8.9, 3.0 Hz, 1H), 5.54 (d, J = 3.1 Hz, 1H), 4.57 (t, J = 6.0 Hz, 1H), 4.05 – 4.00 (m, 1H), 3.90 (t, J = 10.8 Hz, 1H), 3.68 – 3.61 (m, 1H), 3.53 – 3.45 (m, 1H), 3.44 – 3.35 (m, 4H), 3.35 – 3.26 (m, 3H), 2.94 (d, J = 7.2 Hz, 2H), 2.93 – 2.87 (m, 1H), 2.81 (dt, J = 11.0, 4.5 Hz, 1H), 2.42 (dd, J = 13.2, 11.2 Hz, 1H), 2.19 (p, J = 6.9 Hz, 2H), 1.20 – 1.08 (m, 1H), 0.72 – 0.64 (m, 2H), 0.41 – 0.34 (m, 2H).

***N*-((*cis*-7-(Azetidin-1-yl)-8-benzyl-5,6,7,8-tetrahydronaphthalen-2-yl)methyl)-1-methyl-1*H*-imidazole-4-sulfonamide (43a)**. Step 1. A suspension of *cis*-1-benzyl-7-methoxy-1,2,3,4-tetrahydronaphthalen-2-amine (5.6 g, 21 mmol) in hydrobromic acid (40 mL of 48%) was stirred at 115-120°C for 1 h. The solvent was removed in vacuo, the residue collected in H_2O, and the pH adjusted to ~7.0. This mixture was extracted with EtOAc (2 x 150 mL) and filtered. The solids were dried affording a first batch of *cis*-7-amino-8-benzyl-5,6,7,8-tetrahydronaphthalen-2-ol (1.26 g). The EtOAc layer was dried over $MgSO_4$, filtered, and concentrated to obtain a second batch of desired product (4.18 g).

Step 2. To a solution of *cis*-7-amino-8-benzyl-5,6,7,8-tetrahydronaphthalen-2-ol (0.92 g, 3.6 mmol) in THF (20 mL) was charged di-t-butyl dicarbonate (0.73 g, 3.3 mmol). A solution of triethylamine (1.05 g, 10.3 mmol) in THF (10 mL) was slowly added to the reaction. After one hour the mixture was concentrated, the residue dissolved in DCM, which was subsequently extracted with a saturated solution of ammonium chloride and H_2O, dried over $MgSO_4$ and concentrated affording crude *tert*-butyl (*cis*-1-benzyl-7-hydroxy-1,2,3,4-tetrahydronaphthalen-2-yl)carbamate (1.05 g, 2.97 mmol).

Step 3. A cold (-45°C) solution of triflic anhydride (2.75 g, 10.6 mmol) in DCM (100 mL) was slowly treated with a mixture of *tert*-butyl (*cis*-1-benzyl-7-hydroxy-1,2,3,4-tetrahydronaphthalen-2-yl)carbamate (3.45 g, 10.0 mmol) and triethylamine (2.0 g, 20 mmol) in DCM (75 mL). The mixture was stirred at -40°C for 15 minutes and then allowed to warm up to RT. To complete reaction the mixture was cooled again to -45°C, trietylamine (0.30 g, 30 mmol) in DCM and triflic anhydride (0.74 g, 2.6 mmol) in DCM were added. The mixture was stirred at -40°C for 10 minutes then allowed to warm up to RT and stirred overnight, after which the solvent was removed in vacuo. The residue (11 g) was purified on silica gel (DCM) affording *cis*-8-benzyl-7-((*tert*-butoxycarbonyl)amino)-5,6,7,8-tetrahydronaphthalen-2-yl trifluoromethanesulfonate as a solid (3.3 g, 6.8 mmol, 70%).

Step 4. To a suspension of 1,1′-bis(diphenylphosphino)ferrocen (1.1 g, 2.0 mmol) and Tris(dibenzylideneacetone)dipalladium (0.47 g, 0.52 mmol) in 50 mL dimethyl formamide under nitrogen was added *cis*-8-benzyl-7-(*tert*-butoxycarbonylamino)-5,6,7,8-tetrahydronaphthalen-2-yl trifluoromethanesulfonate (5.00 g, 10.3 mmol). The mixture was heated to 100°C followed by addition of zinccyanide (2.42 g, 20.6 mmol). The mixture was stirred at 110°C for 1.5 h then cooled to RT and concentrated. The residue was diluted in EtOAc/H_2O 2:1 (300 mL), filtered, the organic layer separated and the aqueous extracted with EtOAc. The combined organic layers were dried over $MgSO_4$, filtered, concentrated and the residue (8.9 g) purified on silica gel affording *tert*-butyl (*cis*-1-benzyl-7-cyano-1,2,3,4-tetrahydronaphthalen-2-yl)carbamate as an off white solid (1.10 g, 3.03 mmol, 30%).

Step 5. *tert*-butyl (*cis*-1-benzyl-7-cyano-1,2,3,4-tetrahydronaphthalen-2-yl)carbamate (1.1 g, 3.0 mmol) was dissolved in DCM (20 mL) and 5 M hydrochloric acid in *i*PrOH (2 mL) was added. The reaction mixture was stirred at RT for 12 h followed by 4 h at 35°C. The solvent was evaporated in vacuo. H_2O (30 mL) was added and the pH was adjusted to pH 9 using aqueous

saturated sodium bicarbonate solution. The aqueous layer was extracted with DCM. The combined extracts were dried ($MgSO_4$) and the solvent was evaporated in vacuo affording *cis*-7-amino-8-benzyl-5,6,7,8-tetrahydronaphthalene-2-carbonitrile as brown oil (860 mg, 3.28 mmol, 100%). LC−MS (ESI, *m/z*) 263.1 $[M + H]^+$.

Step 6. *cis*-7-amino-8-benzyl-5,6,7,8-tetrahydronaphthalene-2-carbonitrile (860 mg, 3.28 mmol), 1,3-dibromopropane (0.40 mL, 3.9 mmol) and triethylamine (0.91 mL, 6.5 mmol) were dissolved in MeCN (8 mL) and the reaction mixture heated to 120°C in the microwave for 2 h. The solvent was evaporated in vacuo. H_2O (30 mL) and EtOAc (40 mL) were added. The layers were separated and the aqueous layer extracted with EtOAc. The combined organic extracts were dried ($MgSO_4$) and the solvent evaporated in vacuo. The crude product was purified by flash chromatography (silica gel, DCM, MeOH) affording *cis*-7-(azetidin-1-yl)-8-benzyl-5,6,7,8-tetrahydronaphthalene-2-carbonitrile as an off white solid (346 mg, 1.14 mmol, 38%). LC−MS (ESI, *m/z*) 303.1 $[M + H]^+$.

Step 7. *cis*-7-(azetidin-1-yl)-8-benzyl-5,6,7,8-tetrahydronaphthalene-2-carbonitrile (340 mg, 1.12 mmol) was dissolved in dry MeOH (20 mL) under a nitrogen atmosphere. Raney nickel (900 mg, 3.36 mmol) was added under nitrogen and the reaction mixture stirred at RT for 48 h under an atmosphere of hydrogen. MeOH (20 mL) and DCM (30 mL) were added. After stirring at RT for 20 minutes the catalyst was removed by filtration and the solvent evaporated in vacuo to obtain (*cis*-7-(azetidin-1-yl)-8-benzyl-5,6,7,8-tetrahydronaphthalen-2-yl)methanamine as a brown oil (338 mg, 1.10 mmol, 98%). LC−MS (ESI, *m/z*) 307.2 $[M + H]^+$.

Step 8. (*cis*-7-(azetidin-1-yl)-8-benzyl-5,6,7,8-tetrahydronaphthalen-2-yl)methanamine (250 mg, 0.816 mmol) and DMAP (199 mg, 1.63 mmol) were dissolved in DCM (18 mL). 1-Methyl-1*H*-imidazole-4-sulfonyl chloride (147 mg, 0.816 mmol) dissolved in DCM (2 mL) was added dropwise. The reaction mixture was stirred at RT for 12 h. The reaction mixture was diluted with

DCM (20 mL) and washed successively with saturated ammonium chloride (3x 15 mL) and H_2O (2x 10 mL). The organic phase was dried ($MgSO_4$) and the solvent was evaporated in vacuo. The crude product was purified by flash chromatography (silica gel, DCM, MeOH) affording compound **43a** as a white solid (64 mg, 0.142 mmol, 17%). LC−MS (ESI, *m/z*) 451.2 $[M + H]^+$, ^{1}H NMR (500 MHz, DMSO-d_6) δ (ppm) 7.76 (s, 1H), 7.68 – 7.62 (m, 2H), 7.23 (t, J = 7.4 Hz, 2H), 7.17 (t, J = 7.2 Hz, 1H), 7.03 – 6.96 (m, 2H), 6.93 (d, J = 7.4 Hz, 2H), 6.04 (s, 1H), 3.76 – 3.71 (m, 1H), 3.69 (s, 3H), 3.63 (dd, J = 14.7, 6.3 Hz, 1H), 3.28 – 3.16 (m, 5H), 2.91 – 2.67 (m, 3H), 2.44 – 2.35 (m, 1H), 2.26 – 2.18 (m, 1H), 2.00 (p, J = 6.7 Hz, 2H), 1.74 – 1.66 (m, 1H), 1.59 – 1.46 (m, 1H).

***N*-((*cis*-7-(Azetidin-1-yl)-8-benzyl-5,6,7,8-tetrahydronaphthalen-2-yl)methyl)propane-1-sulfonamide (43b)**. Compound **43b** (54 mg, 54% for last step from (*cis*-7-(azetidin-1-yl)-8-benzyl-5,6,7,8-tetrahydronaphthalen-2-yl)methanamine 75 mg, 0.245 mmol) was prepared according to example **43a** by using *n*-propane-1-sulfonyl chloride in place of 1-methyl-1*H*-imidazole-4-sulfonyl chloride. White solid. ^{1}H NMR (500 MHz, DMSO-d_6) δ (ppm) 7.29 – 7.25 (m, 1H), 7.25 – 7.20 (m, 2H), 7.20 – 7.14 (m, 1H), 7.06 (s, 2H), 6.93 (d, J = 7.3 Hz, 2H), 6.13 (s, 1H), 3.80 (dd, J = 14.7, 6.3 Hz, 1H), 3.74 (dd, J = 14.7, 6.2 Hz, 1H), 3.29 – 3.24 (m, 1H), 3.23 – 3.15 (m, 4H), 2.92 – 2.67 (m, 5H), 2.41 – 2.34 (m, 1H), 2.24 (dd, J = 13.2, 9.8 Hz, 1H), 2.03 – 1.94 (m, 2H), 1.75 – 1.66 (m, 1H), 1.60 – 1.48 (m, 3H), 0.87 (t, J = 7.4 Hz, 3H).

***N*-(2-(((7*S*,8*R*)-8-Benzyl-7-(methylamino)-5,6,7,8-tetrahydronaphthalen-2-yl)oxy)ethyl)-1-cyclopropylmethanesulfonamide hydrochloride ((7*S*,8*R*)-44)**. Step 1. The racemate of ethyl (*cis*-1-benzyl-7-(2-((cyclopropylmethyl)sulfonamido)ethoxy)-1,2,3,4-tetrahydronaphthalen-2-yl)carbamate (400 mg, 0.822 mmol, obtained according to

representative example **9** steps 1-7 by using (bromomethyl)benzene in place of 4-(bromomethyl)-1,2-dichlorobenzene and cyclopropylmethanesulfonyl chloride in place of 1-methyl-1*H*-imidazole-4-sulfonyl chloride) was separated by chiral chromatography on Chiracel AD 5 x 50 cm (*n*-heptane/EtOH/*tert*-butanol 80:15:5, 100 mL/min) isocratic (t_R [min] = 47.74, 56.27). (-) Enantiomer (t_R = 47.74 min): white solid (125 mg, 0.257 mmol).

Step 2. To a solution of (-) ethyl ((1*R*,2*S*)-1-benzyl-7-(2-((cyclopropylmethyl)sulfonamido)ethoxy)-1,2,3,4-tetrahydronaphthalen-2-yl)carbamate (135 mg, 0.277 mmol) in THF (300 mL), was added $LiAlH_4$ (0.55 mL, 1M in THF, 0.56 mmol) at RT and the mixture was stirred for 3h under reflux. The reaction was cooled to RT, poured onto ice and extracted with EtOAc. The organic layer was washed with brine, dried over $MgSO_4$, concentrated and the residue converted to hydrochloride HCl (5M in *i*PrOH) affording *N*-(2-(((7*S*,8*R*)-8-benzyl-7-(methylamino)-5,6,7,8-tetrahydronaphthalen-2-yl)oxy)ethyl)-1-cyclopropylmethanesulfonamide hydrochloride ((**7*S*,8*R***)-**44**) as white solid (102 mg, 0.219 mmol, 78%). $[\alpha]^{25}_D$ -80.5 (*c* 0.19, MeOH). LC−MS (ESI, *m/z*) 429.2 $[M + H]^+$, ^{1}H NMR (500 MHz, DMSO-d_6) δ (ppm) 9.46 (s, 2H), 7.27 (t, J = 7.3 Hz, 2H), 7.24 – 7.18 (m, 2H), 7.10 (d, J = 7.3 Hz, 2H), 7.02 (d, J = 8.5 Hz, 1H), 6.67 (dd, J = 8.5, 2.6 Hz, 1H), 5.48 (d, J = 2.6 Hz, 1H), 3.57 (dt, J = 10.9, 5.9 Hz, 1H), 3.46 – 3.39 (m, 1H), 3.25 – 3.19 (m, 1H), 3.16 – 3.09 (m, 2H), 2.99 (dd, J = 17.3, 7.3 Hz, 1H), 2.92 (d, J = 7.2 Hz, 2H), 2.82 (dt, J = 17.9, 8.9 Hz, 1H), 2.71 (s, 3H), 2.47 – 2.39 (m, 1H), 2.23 – 2.15 (m, 1H), 2.10 – 1.98 (m, 1H), 1.02 – 0.93 (m, 1H), 0.57 – 0.49 (m, 2H), 0.33 – 0.25 (m, 2H).

***N*-((*cis*-8-Benzyl-7-(methylamino)-5,6,7,8-tetrahydronaphthalen-2-yl)methyl)propane-1-sulfonamide hydrochloride (46)**. Compound **46** (590 mg, 43% for last step from *tert*-butyl (*cis*-1-benzyl-7-(propylsulfonamidomethyl)-1,2,3,4-tetrahydronaphthalen-2-yl)carbamate 1.24 g, 2.62 mmol) was prepared according to example **43a**

from *tert*-butyl (*cis*-1-benzyl-7-cyano-1,2,3,4-tetrahydronaphthalen-2-yl)carbamate following steps 7 – 8 by using *n*-propane-1-sulfonyl chloride in place of 1-methyl-1*H*-imidazole-4-sulfonyl chloride. The so obtained 7-*tert*-butyl-carbamate was converted to **46** by reduction with $LiAlH_4$ according to step 2 of compound **44**. White solid. LC−MS (ESI, *m/z*) 387.2 $[M + H]^+$, ^1H NMR (400 MHz, DMSO-d_6) δ (ppm) 9.10 (s, 2H), 7.33 – 7.18 (m, 4H), 7.11 (d, J = 1.1 Hz, 2H), 7.07 – 6.97 (m, 2H), 5.96 (s, 1H), 3.75 (dd, J = 14.9, 6.3 Hz, 1H), 3.68 (dd, J = 14.9, 6.3 Hz, 1H), 3.48 – 3.38 (m, 1H), 3.14 (dd, J = 13.1, 3.2 Hz, 1H), 3.10 – 3.02 (m, 1H), 2.93 – 2.81 (m, 1H), 2.76 (dd, J = 7.7, 2.7 Hz, 1H), 2.72 (s, 3H), 2.46 – 2.41 (m, 1H), 2.25 – 2.15 (m, 1H), 2.10 – 1.96 (m, 1H), 1.56 (h, J = 7.5 Hz, 2H), 0.88 (t, J = 7.5 Hz, 3H).

***N*-(2-((*cis*-8-Benzyl-7-((2,2,2-trifluoroethyl)amino)-5,6,7,8-tetrahydronaphthalen-2-yl)oxy)ethyl)-1-methyl-1*H*-imidazole-4-sulfonamide (48)**. Step 1. To a solution of **20k** (101 mg, 0.229 mmol) in THF (3 mL) was added under nitrogen triethylamine (218 mg, 2.15 mmol) and trifluoroacetic anhydride (232 mg, 1.11 mmol). The mixture was stirred overnight, diluted with diethyl ether/EtOAc and subsequently washed with a solution of ammonium chloride and H_2O. The organic layer were dried over $MgSO_4$ and concentrated affording N-(*cis*-1-benzyl-7-(2-((1-methyl-1*H*-imidazole)-4-sulfonamido)ethoxy)-1,2,3,4-tetrahydronaphthalen-2-yl)-2,2,2-trifluoroacetamide as white solid (124 mg) which was used without further purification. LC−MS (ESI, *m/z*) 537.2 $[M + H]^+$.

Step 2. To a solution of crude N-(*cis*-1-benzyl-7-(2-((1-methyl-1*H*-imidazole)-4-sulfonamido)ethoxy)-1,2,3,4-tetrahydronaphthalen-2-yl)-2,2,2-trifluoroacetamide (123 mg, 0.229 mmol) in 5 mL THF was added under nitrogen borane dimethyl sulfide complex (1.72 mL, 2M in THF, 3.44 mmol). The mixture was stirred overnight at 60°C. Additional borane dimethyl sulfide complex (1.72 mL, 2M in THF, 3.44 mmol) was added and the reaction was stirred for further 12 h at 60°C. The mixture was cooled to RT, and stirred overnight at RT after addition of 5 mL

MeOH. Then the reaction was concentrated, the residue dissolved in diethyl ether/EtOAc and extracted with diluted $NaHCO_3$ solution. The organic layer was dried over $MgSO_4$, filtered, concentrated and the residue purified by chromatography on silicagel (DCM/MeOH 19:1) affording compound **48** as oil (41 mg, 0.075 mmol, 30% over last two steps). LC−MS (ESI, *m/z*) 523.2 $[M + H]^+$, ^1H NMR (500 MHz, DMSO-d_6) δ (ppm) 7.76 (s, 1H), 7.71 (s, 1H), 7.59 (t, J = 5.9 Hz, 1H), 7.24 (t, J = 7.4 Hz, 2H), 7.16 (t, J = 7.4 Hz, 1H), 7.06 (d, J = 7.4 Hz, 2H), 6.96 (d, J = 8.4 Hz, 1H), 6.60 (dd, J = 8.3, 2.6 Hz, 1H), 5.87 (d, J = 2.7 Hz, 1H), 3.71 – 3.65 (m, 1H), 3.68 (s, 3H), 3.54 (dt, J = 10.3, 6.1 Hz, 1H), 3.43 – 3.37 (m, 1H), 3.22 (dd, J = 13.3, 4.3 Hz, 1H), 3.09 – 3.00 (m, 3H), 2.95 – 2.80 (m, 2H), 2.72 (dt, J = 17.0, 8.6 Hz, 1H), 2.47 – 2.39 (m, 2H), 1.83 – 1.72 (m, 2H).

***N*-(1-((7*S*,8*R*)-7-(Azetidin-1-yl)-8-benzyl-5,6,7,8-tetrahydronaphthalen-2-yl)azetidin-3-yl)-1-cyclopropylmethanesulfonamide ((7*S*,8*R*)-51a).** Step 1. A solution of (7*S,*8*R*)-7-(azetidin-1-yl)-8-benzyl-5,6,7,8-tetrahydronaphthalen-2-ol (**(7*S*,8*R*)-27a**, step 4) (0.800 g, 2.73 mmol) and pyridine (0.55 mL, 6.82 mmol) in DCM (45 mL) was cooled under nitrogen to 0°C. Trifluoromethanesulfonic anhydride (3.3 mL, 3.3 mmol, 1M in DCM) was added dropwise and the reaction stirred under cooling for 0.5 h. Aqueous bicarbonate solution was added, the aqueous phase separated, and extracted with DCM once. The combined organic layers were dried over $MgSO_4$, filtered, and evaporated to dryness. The crude material was purified by flash chromatography to yield (7*S,*8*R*)-7-(azetidin-1-yl)-8-benzyl-5,6,7,8-tetrahydronaphthalen-2-yl trifluoromethanesulfonate (1.1 g, 2.7 mmol, 99%). LC−MS (ESI, *m/z*) 426.2 $[M + H]^+$.

Step 2. To a solution of (7*S*,8*R*)-7-(azetidin-1-yl)-8-benzyl-5,6,7,8-tetrahydronaphthalen-2-yl trifluoromethanesulfonate (260 mg, 0.611 mmol) in toluene (5 mL) under nitrogen atmosphere, were added palladium(ll)acetate (20.6 mg, 0.092 mmol), dicyclohexyl(2',4',6'-triisopropyl-(l,1'-

biphenyl)-2-yl)phosphane (XPhos, 87 mg, 0.183 mmol) and cesium carbonate (600 mg, 1.8 mmol), and the resulting mixture was stirred at 95°C for 15 min. Then *tert*-butyl azetidin-3-ylcarbamate hydrochloride (153 mg, 0.733 mmol) was added and the reaction mixture stirred for 1 h at 115°C. The reaction mixture was allowed to cool at RT and diluted with EtOAc. The organic layer was washed with H_2O and brine. The combined H_2O layers were back extracted with EtOAc once. The combined organic phases were dried over $MgSO_4$, filtered, and evaporated. The crude material was purified by flash chromatography on silica gel affording *tert*-butyl (1-((7*S*,8*R*)-7-(azetidin-1-yl)-8-benzyl-5,6,7,8-tetrahydronaphthalen-2-yl)azetidin-3-yl)carbamate (248 mg, 0.554 mmol, 91%). LC−MS (ESI, *m/z*) 448.3 $[M + H]^+$.

Step 3. To a solution of *tert*-butyl (1-((7*S*,8*R*)-7-(azetidin-1-yl)-8-benzyl-5,6,7,8-tetrahydronaphthalen-2-yl)azetidin-3-yl)carbamate (220 mg, 0.491 mmol) in DCM (5 mL), was added TFA (0.5 mL, 6.5 mmol) the reaction mixture stirred at RT for 5 hours. The solvents were evaporated. The residue was dissolved in H_2O and washed with methyl-*tert*-butyl ether. The H_2O layer was separated, followed by aqueous sodium hydrogen carbonate solution to adjust pH 8. The mixture was extracted with DCM, the organic layer was dried over $MgSO_4$ filtered and concentrated. The crude material was purified by flash chromatography on silica gel affording 1-((7*S,*8*R*)-7-(azetidin-1-yl)-8-benzyl-5,6,7,8-tetrahydronaphthalen-2-yl)azetidin-3-amine (169 mg, 0.486 mmol, 99%). LC−MS (ESI, *m/z*) 348.2 $[M + H]^+$.

Step 4. The desired product *N*-(1-((7*S*,8*R*)-7-(azetidin-1-yl)-8-benzyl-5,6,7,8-tetrahydronaphthalen-2-yl)azetidin-3-yl)-1-cyclopropylmethanesulfonamide ((**7*S*,8*R***)-**51a**) was subsequently obtained from 1-((7*S,*8*R*)-7-(azetidin-1-yl)-8-benzyl-5,6,7,8-tetrahydronaphthalen-2-yl)azetidin-3-amine (59 mg, 0.170 mmol) according to compound **9**, step 7 by using cyclopropylmethanesulfonyl chloride in place of *n*-propane-1-sulfonyl chloride. White solid (58 mg, 0.125 mmol, 73%), $[\alpha]^{25}_D$ -99.0 (*c* 0.445, MeOH), LC−MS (ESI, *m/z*) 466.2 $[M + H]^+$, ^1H

NMR (600 MHz, Chloroform-*d*) δ (ppm) 7.25 – 7.22 (m, 2H), 7.20 – 7.16 (m, 1H), 6.97 – 6.93 (m, 3H), 6.23 (dd, J = 8.1, 2.5 Hz, 1H), 5.14 (d, J = 2.4 Hz, 1H), 4.60 (d, J = 9.6 Hz, 1H), 4.31 – 4.24 (m, 1H), 3.91 (t, J = 7.4 Hz, 1H), 3.81 (t, J = 7.4 Hz, 1H), 3.37 – 3.30 (m, 6H), 3.18 (dd, J = 7.7, 5.6 Hz, 1H), 2.92 (d, J = 7.2 Hz, 2H), 2.90 – 2.84 (m, 2H), 2.80 – 2.72 (m, 1H), 2.51 – 2.46 (m, 1H), 2.30 (dd, J = 13.1, 11.3 Hz, 1H), 2.18 – 2.12 (m, 2H), 1.82 – 1.75 (m, 1H), 1.71 – 1.62 (m, 1H), 1.16 – 1.09 (m, 1H), 0.75 – 0.70 (m, 2H), 0.42 – 0.37 (m, 2H).

***N*-(1-(*cis*-3-(Azetidin-1-yl)-4-benzylchroman-6-yl)azetidin-3-yl)-1-cyclopropylmethanesulfonamide (51b)**. Compound **51b** (66 mg, 0.141 mmol, 82% for last step from 1-(*cis*-3-(azetidin-1-yl)-4-benzylchroman-6-yl)azetidin-3-amine 60 mg, 0.172 mmol) was prepared according to example (**7*S*,8*R*)-51a** by using *cis*-3-(azetidin-1-yl)-4-benzylchroman-6-ol (**36a**, step 10) in place of (7*S*,8*R*)-7-(azetidin-1-yl)-8-benzyl-5,6,7,8-tetrahydronaphthalen-2-ol. White solid. LC−MS (ESI, *m/z*) 468.2 $[M + H]^+$, ^{1}H NMR (600 MHz, Chloroform-*d*) δ (ppm) 7.26 (m, 2H), 7.24 – 7.19 (m, 1H), 7.05 – 6.99 (m, 2H), 6.68 (d, J = 8.7 Hz, 1H), 6.23 (dd, J = 8.6, 2.8 Hz, 1H), 5.14 (d, J = 2.8 Hz, 1H), 4.62 (d, J = 9.6 Hz, 1H), 4.30 – 4.22 (m, 1H), 4.03 – 3.98 (m, 1H), 3.93 – 3.88 (m, 1H), 3.87 (t, J = 7.2 Hz, 1H), 3.80 (t, J = 7.2 Hz, 1H), 3.45 – 3.36 (m, 4H), 3.32 – 3.27 (m, 2H), 3.17 (dd, J = 7.5, 5.7 Hz, 1H), 2.92 (d, J = 7.2 Hz, 2H), 2.91 – 2.88 (m, 1H), 2.84 – 2.77 (m, 1H), 2.42 (t, J = 12.2 Hz, 1H), 2.23 – 2.15 (m, 2H), 1.16 – 1.08 (m, 1H), 0.75 – 0.69 (m, 2H), 0.42 – 0.36 (m, 2H).

***N*-(1-((7*S*,8*R*)-7-(Azetidin-1-yl)-8-benzyl-5,6,7,8-tetrahydronaphthalen-2-yl)azetidin-3-yl)propane-1-sulfonamide ((7*S*,8*R*)-51c)**. Compound **51c** (3.20 g, 7.05 mmol, 82% for last step from 1-((7*S*,8*R*)-7-(azetidin-1-yl)-8-benzyl-5,6,7,8-tetrahydronaphthalen-2-yl)azetidin-3-amine 3.0 g, 8.6 mmol) was prepared according to example **(7*S*,8*R*)-51a** by using *n*-propane-1-sulfonyl chloride in place of cyclopropylmethanesulfonyl

chloride. White solid. $[\alpha]^{25}_{D}$ -223.7 (*c* 0.089, MeOH), LC−MS (ESI, *m/z*) 454.2 $[M + H]^+$, ^{1}H NMR (600 MHz, Chloroform-*d*) δ (ppm) 7.25 – 7.21 (m, 2H), 7.20 – 7.16 (m, 1H), 6.98 – 6.93 (m, 3H), 6.23 (dd, J = 8.1, 2.5 Hz, 1H), 5.14 (d, J = 2.5 Hz, 1H), 4.52 (d, J = 9.7 Hz, 1H), 4.25 – 4.18 (m, 1H), 3.90 (t, J = 7.4 Hz, 1H), 3.80 (t, J = 7.4 Hz, 1H), 3.39 – 3.29 (m, 6H), 3.17 (dd, J = 7.7, 5.5 Hz, 1H), 2.98 – 2.94 (m, 2H), 2.91 – 2.84 (m, 2H), 2.76 (ddd, J = 17.2, 11.8, 7.2 Hz, 1H), 2.52 – 2.45 (m, 1H), 2.30 (dd, J = 13.0, 11.4 Hz, 1H), 2.19 – 2.12 (m, 2H), 1.88 – 1.76 (m, 3H), 1.72 – 1.63 (m, 1H), 1.08 (t, J = 7.4 Hz, 3H).

***N*-(1-(*cis*-3-(Azetidin-1-yl)-4-benzylchroman-6-yl)azetidin-3-yl)propane-1-sulfonamide (51d)**. Compound **51d** (67 mg, 0.147 mmol, 86% for last step from 1-(*cis*-3-(azetidin-1-yl)-4-benzylchroman-6-yl)azetidin-3-amine 60 mg, 0.172 mmol) was prepared according to example (**7*S*,8*R*)-51a** by using *cis*-3-(azetidin-l-yl)-4-benzylchroman-6-ol (**36a**, step 10) in place of (7*S,*8*R*)-7-(azetidin-l-yl)-8-benzyl-5,6,7,8-tetrahydronaphthalen-2-ol and *n*-propane-1-sulfonyl chloride in place of cyclopropylmethanesulfonyl chloride. White solid. LC−MS (ESI, *m/z*) 456.2 $[M + H]^+$, ^{1}H NMR (600 MHz, Chloroform-*d*) δ (ppm) 7.26 (s, 2H), 7.23 – 7.19 (m, 1H), 7.03 – 7.00 (m, 2H), 6.68 (d, J = 8.6 Hz, 1H), 6.23 (dd, J = 8.6, 2.8 Hz, 1H), 5.13 (d, J = 2.8 Hz, 1H), 4.56 (d, J = 9.8 Hz, 1H), 4.24 – 4.17 (m, 1H), 4.03 – 3.99 (m, 1H), 3.92 – 3.88 (m, 1H), 3.87 (t, J = 7.3 Hz, 1H), 3.79 (t, J = 7.3 Hz, 1H), 3.44 – 3.35 (m, 4H), 3.31 – 3.26 (m, 2H), 3.17 – 3.13 (m, 1H), 2.98 – 2.94 (m, 2H), 2.94 – 2.88 (m, 1H), 2.84 – 2.78 (m, 1H), 2.45 – 2.39 (m, 1H), 2.23 – 2.16 (m, 2H), 1.88 – 1.79 (m, 2H), 1.08 (t, J = 7.5 Hz, 3H).

***N*-((*R*)-1-((7*S*,8*R*)-7-(Azetidin-1-yl)-8-benzyl-5,6,7,8-tetrahydronaphthalen-2-yl)-2-oxopyrrolidin-3-yl)propane-1-sulfonamide fumarate (*N*-(*R*), (7*S*,8*R*)-(53)**. Step 1. To a solution of (7*S,*8*R*)-7-(azetidin-1-yl)-8-benzyl-5,6,7,8-tetrahydronaphthalen-2-ol (5.0 g, 17.0 mmol) in DCM (50 mL) was added pyridine (3.5 mL, 43.3 mmol) at RT. The

solution was cooled to 0°C and a solution of trifluoromethanesulfonic acid anhydride in DCM (1M, 18.75 mL, 18.75 mmol) was added dropwise. The reaction mixture was stirred at 0°C for additional 30 min. Saturated aqueous ammonium chloride solution (15 mL) was added at 0°C and the aqueous phase extracted with DCM. The organic layer was washed with brine, dried over $MgSO_4$ and concentrated. The crude product was purified by flash chromatography (silica, gradient 0-10% MeOH in DCM): yellow solid (5.35 g, 12.6 mmol, 74%).

Step 2. In a microwave vessel *tert*-butyl (*R*)-(2-oxopyrrolidin-3-yl)carbamate (235 mg, 1.17 mmol), (7*S*,8*R*)-7-(azetidin-1-yl)-8-benzyl-5,6,7,8-tetrahydronaphthalen-2-yl trifluoromethanesulfonate (500 mg, 1.17 mmol), cesium carbonate (536 mg, 1.64 mmol) and dicyclohexyl(2',4',6'-triisopropyl-3,6-dimethoxy-(1,1'-biphenyl)-2-yl)phosphane (56.8 mg, 0.106 mmol) were suspended in toluene (10 mL). Under argon allylpalladium(II) chloride (12.9 mg, 0.035 mmol) was added, and the reaction mixture heated to 140°C for two hours. After cooling to RT the reaction mixture was diluted with DCM and washed successively with H_2O and brine. The organic layer was dried over $MgSO_4$ and concentrated. The crude product was purified by flash chromatography (silica, gradient 0 to 10% MeOH in DCM): yellow solid (200 mg, 0.421 mmol, 36%).

Step 3. To a solution of *tert*-butyl ((*R*)-1-((7*S*,8*R*)-7-(azetidin-1-yl)-8-benzyl-5,6,7,8-tetrahydronaphthalen-2-yl)-2-oxopyrrolidin-3-yl)carbamate (200 mg, 0.421 mmol) in DCM (5 mL) TFA (0.50 mL, 6.49 mmol) was added and the reaction mixture stirred overnight at RT. After dilution with DCM the reaction mixture was treated with 2N aqueous NaOH until pH 11 was reached. Phases were separated and the organic layer concentrated. The crude product was directly used for the next step without further purification: yellow oil (70 mg, 0.186 mmol, 44%).

Step 4. To a solution of (*R*)-3-amino-1-((7*S*,8*R*)-7-(azetidin-1-yl)-8-benzyl-5,6,7,8-tetrahydronaphthalen-2-yl)pyrrolidin-2-one (35 mg, 0.093 mmol) in DCM (3 mL) were added

DMAP (15 mg, 0.123 mmol) and 1-propanesulfonyl chloride (12 µL, 0.108 mmol). The reaction mixture was stirred at RT overnight. The reaction mixture was diluted with H_2O and phases were separated. The organic phase was concentrated and the crude product was purified by flash chromatography (silica, gradient 0 to 10% MeOH in DCM). The free base (25 mg, 0.052 mmol) was dissolved in MeOH (2.5 mL) and 1 equivalent of fumaric acid (5.9 mg, 0.051 mmol) was added. Most of the MeOH was removed and the product precipitated by addition of MTB. The product was removed by filtration in dried in vacuo: yellow solid (15 mg, 0.025 mmol, 27%). $[\alpha]^{25}_{D}$ +3.2 (*c* 1.25, MeOH) LC−MS (ESI, m/z) 482.4 $[M + H]^+$, ^{1}H NMR (600 MHz, DMSO- d_6) δ (ppm) 7H partially covered by DMSO signal, 13.05 (s, 1H), 7.71 (ddd, J = 13.9, 8.4, 2.2 Hz, 1H), 7.63 (d, J = 9.0 Hz, 1H), 7.32 – 7.21 (m, 2H), 7.21 – 7.15 (m, 1H), 7.13 – 7.07 (m, 1H), 7.01 – 6.87 (m, 2H), 6.60 (s, 2H), 6.06 (m, 1H), 4.16 (dt, J = 10.5, 8.8 Hz, 1H), 3.21 – 3.04 (m, 3H), 2.95 – 2.83 (m, 2H), 2.75 (ddt, J = 17.7, 11.0, 5.1 Hz, 1H), 2.34 (dddd, J = 12.1, 8.3, 6.7, 1.7 Hz, 1H), 2.29 – 2.19 (m, 1H), 2.03 (p, J = 6.9 Hz, 2H), 1.89 – 1.63 (m, 4H), 1.61 – 1.52 (m, 1H), 0.98 (t, J = 7.4 Hz, 3H).

Biology/DMPK. Unless stated otherwise the chemicals used for the test systems (reagents, salts, buffers, antibiotics, cell media, etc) were purchased from Sigma-Aldrich (St. Louis, MO, USA) or Thermo Fisher Scientific (Schwerte, Germany or Waltham, Mass, USA). For the animal experiments the experimental procedures were approved by AbbVie's Animal Welfare Office and were performed in accordance with the German national guidelines as well as recommendations and policies of the U.S. National Institutes of Health "Principles of Laboratory Animal Care" (1996 edition). Animal housing and experiments were conducted in the facilities accredited by the Association for Assessment and Accreditation of Laboratory Animal Care International (AAALAC).

[^{3}H]N-methyl-SSR504734 Radioligand Binding Assays. Radioligand binding to human GlyT1c transporter expressing membranes was measured in duplicate in a total volume of 200 µL in 96-well plates. To 100 µL of membrane suspension in assay buffer (120 mM NaCl, 2 mM KCl, 10 mM HEPES, 1 mM $MgCl_2$, and 1 mM $CaCl_2$, pH 7.5), 80 µL of [^{3}H]N-methyl-SSR504734[13] was added in assay buffer, yielding a final membrane protein concentration of 50 µg/mL. In competition experiments, 10 µL of buffer or unlabeled compound solution were added. The final DMSO concentration was 1% in all cases. Nonspecific binding was determined in the presence of 10 µM SSR504734 (4). After incubation at RT for 1 h, the incubation mixture was harvested (Tomtec Mach III U Harvester) through 96-well GF/B filter plates (Perkin- Elmer Life and Analytical Sciences, Waltham, MA), presoaked for 1 h with 40 µL per well of 0.1% polyethylenimine. After washing twice with ice-cold buffer (50 mM Tris-HCI, pH 7.4), plates were dried and 35 µL of scintillator (BetaplateScint; PerkinElmer Life and Analytical Sciences) were added per well. The radioactivity was determined by liquid scintillation spectrometry in a MicroBeta (PerkinElmer Life and Analytical Sciences) plate counter.

Data Analysis. For binding of [^{3}H]N-methyl-SSR504734 to cell membranes, the calculation of the IC_{50} values from the displacement binding was performed by iterative nonlinear regression analysis adapted from the Ligand program.[47] Radioligand displacement curves in the presence of tested compounds were fitted using a one-site model. Apparent K_i values were calculated from the IC_{50} values and the Kd of 2.5 nM obtained from saturation binding experiments using the Cheng-Prusoff equation.[48]

Functional expression in *Xenopus* oocytes. Expression and functional evaluation of GlyT1 was performed as described previously.[13] Female *Xenopus laevis* (Nasco, Fort Atkinson, WI), were anesthetized in solution with 0.2% Tricaine (Sigma, St. Louis, MO) and 2 g/l sodium hydrogen carbonate (Sigma), ovary lobes were removed, and oocytes were released from the

follicle tissue with collagenase (type I, 2 mg/mL for 2 h; Roche Applied Science, Mannheim, Germany). Stage V and VI oocytes were selected by hand under a binocular microscope injected 20 nL of cDNA into the nucleus, or 50 nL of prepared cRNA solution into the cytoplasm with GlyT1c expressed in the plasmid pGemHeJuel,[49] and incubated at 18°C in Barth Medium with gentamycin for 3-5 days. The membrane current in whole oocytes was measured through two-electrode voltage clamp (TEVC) employing two microelectrodes filled with 1.5 M potassium acetate and 0.1 M potassium chloride with a voltage-clamp amplified (TEC 03X, npi electronics, Tamm, Germany). Alternatively, a robotic measurement system was used (Roboocyte, multichannel systems, Reutlingen, Germany). The measurement chamber was continuously perfused with frog Ringer solution. Compounds were dissolved in this buffer, and the final DMSO concentration was 1% in all cases. To test the surmountability of GlyT1 inhibition, oocytes were voltage clamped at -60 mV, stimulated with glycine (10 μM or 3 mM) for 1 min, and the compounds added to the respective glycine solution for 3 min. At the end of this time period, the relative current, compared to non-inhibited at the same timepoint was determined. Data were repeated in independent experiments at least 4 times (4-7). Data analysis was performed by the CellWorks Software, the software from the Roboocyte robotic system and subsequent evaluation with GraphPad Prism (GraphPad Software, La Jolla, CA, USA). Results were compared with t-test.

Determination of ADME parameters. ADME parameters were determined according to protocols described previously.[50]

Microsomal Stability: Analogs (0.5 μM) were incubated on a Tecan pipetting station (TECAN Freedom EVO SN 625 – 384 Head; Tecan Group AG, Mennerland Switzerland) with rat (BD Gentest, Heidelberg, Germany) or human (Xenotech, Pfungstadt, Germany) microsomes (0.25 mg/mL) in 50mM potassium-phosphate-buffer (pH 7,4), 37°C for 0, 5, 10, 15, 20 and 30

minutes in the presence of NADPH (Chem-Impex, Wood Dale, IL, USA) in 384-well plaes (Corning GmbH, Kaiserslautern, Germany). The experiments were stopped with 1:1 CH_3CN:MeOH and analyzed by LC-MS/MS (AB Sciex API 4000, 5000 or 6500; AB Sciex Germany GmbH, Darmstadt, Germany) employing Waters Acquity HPLC systems (Waters GmbH, Eschborn Germany). An internal standard of carbutamide was used. The microsomal clearance was calculated by non-linear regression of % compound remaining over time. mCLint (μL/min/mg)= k * 1000/(0.25).

CYP induction: cryopreserved human hepatocytes (Celsis/IVT, Thermo Fisher Scientific, Waltham, Mass, USA) were plated at ~0.75 million cells/mL on collagen-coated 96-well culture plates and overlaid with GelTrex™ (Thermo Fisher Scientific, Waltham, Mass, USA) after 4-6 hours of plating. Cells were incubated overnight, then treated with the test articles at different concentrations (1, 3, 10, 30 μM), the respective prototypical inducers (500 μM omeprazole for CYP1A2, 500 μM phenytoin for CYP2B6 and 50 μM rifampin for CYP3A4 and 2Cs), vehicle control (0.1% DMSO) and negative control (50 μM probenecid for all the test genes) in incubation medium with 0.1% DMSO for 48 hours with daily change of treatment media. After 48 hours, the RNA was purified using MagMAX™ Express 96 RNA Isolation System (Life Technologies, Thermo Fisher Scientific, Waltham, Mass, USA), cDNA was synthesized, and RT-PCR was performed. The results were analyzed by calculating the fold-change of CYP mRNA induction caused by the test compound compared to the vehicle control (0.1% DMSO) and % of induction of the positive controls.

CYP inhibition: The incubation was performed in human liver microsomes (Xenotech, Pfungstadt, Germany) and consisted of a test article at varying concentrations (0-20 μM), appropriate probe substrate (concentration ~K_m), human liver microsomal protein at defined concentrations, depending on the CYP in question and the reaction read-outs as outlined in more

detail below (Promega, Mannheim, Germany and BD Gentest, Heidelberg, Germany) and NADPH regeneration mixture (BD Gentest, Heidelberg, Germany) in 50 mM phosphate buffer at pH 7.4. Incubation conditions and concentrations of human liver microsomal protein were optimized to ensure the linearity of the reactions. In more detail, BD Gentest (Heidelberg, Germany) Supersomes P450 Inhibition Kit CYP2D6/AMMC, and Promega (Mannheim, Germany) P450-Glo CYP1A2 Assay, P450-Glo CYP2C9 Assay, P450-Glo CYP3A4 Assay detection kits were used. Fluorescent substrates were CYP1A2: Luciferin 1A2-OH, CYP2C9: Luciferin H-OH, CYP2D6: Fluorescent AHMC, CYP3A4: Luciferin IPA-OH and inhibitors for CYP1A2: alpha-napthoflavone, CYP2C9: Sulfaphenazole, CYP2D6: Quinidine, CYP3A4: Ketoconazole. Incubation conditions were the following: CYP1A2: 15min, 37°C; final 0.01 mg/mL HLM (human liver microsomes), 1µM substrate; CYP2C9: 30min, 37°C; final 0.05 mg/mL HLM, 100µM substrate, CYP2D6: 50min, 37°C;final 0.5 mg/mL HLM, 10µM substrate, CYP3A4: 15min, 37°C; final 0.05 mg/mL HLM, 3µM substrate. The concentration of organic solvents used in the incubation was 0.4% DMSO. For each test article, duplicate incubations were performed at all test article concentrations. Fluorescence was measured and the peak area ratios of the metabolite to internal standard observed in the presence of test article, which is compared to the peak area ratios for the vehicle control incubations in order to determine the percent of control activity. IC_{50} curves were calculated with Graph Pad Prism.

CYP phenotyping: CYP and FMO supersomes (CYP2C9, CYP2C8, CYP1A2, CYP2C19, CYP2DD6, CYP3A4, FMO3) were obtained from BD Gentest, Heidelberg, Germany. 0.5 µM of test article was incubated for different periods of time (0, 5, 10, 20, 30, 60 min) with the incubation mix, according to the manufacturer. Samples were drawn and analyzed with LC-MS/MS (AB Sciex API 4000, 5000 or 6500; AB Sciex Germany GmbH, Darmstadt, Germany) employing Waters Acquity HPLC systems (Waters GmbH, Eschborn Germany). Clearance and

half-life was calculated, and the relative contribution of each CYP defined according to standard procedures.

P-gp-Efflux: Madin-Darby canine kidney (MDCK II) epithelial cells, transfected with the MDR1 gene were engineered to have lower expression of canine P-gp as described.[51] The cells encoding human P-gp are grown on transwell inserts and directional differences in cell monolayer permeability of various test compounds are monitored during a 1 h experiment. Specifically, Millicell 96-well insert plates (Merck Chemicals AG, Darmstadt, Germany) were seeded with MDCK-MDR1 cells on Day 1 at a density of 300,000 cells/cm^2. Media was changed on Day 2 and P-gp interaction assay was performed on Day 4 or Day 5. Compounds were diluted to a concentration of 1 mM in DMSO, and the final assay concentration was 1 μM (added 1 μL of stock to 999 μL of Hank's Balanced Salt Solution (HBSS) + glucose) (final concentration of 0.1% DMSO). Cell monolayers were dosed on the apical side (A-to-B direction) or basolateral side (B-to-A direction) at a concentration of 1 μM in HBSS + glucose. Incubations were performed in duplicate at 37°C for one hour. At the end of the incubation, 50 μL aliquots were taken from the receiver chambers and 10 μL aliquots were taken from the donor chambers. Prior to the incubation, aliquots of the donor solution were also taken to determine concentration at time equal zero. All donor solutions (both t = 0 min and t = 60 min) are diluted with HBSS + glucose and LC/MS analysis was performed on all samples. Apparent permeability (P_{app}) values are calculated from area-under- the-curve quantitation from LC-MS/MS (AB Sciex API 4000, 5000 or 6500; AB Sciex Germany GmbH, Darmstadt, Germany) employing Waters Acquity HPLC systems (Waters GmbH, Eschborn Germany). analyses. The calculation was $P_{app}=(\Delta Q/\Delta t)*(1/(A*C_o))$ where ΔQ is amount of drug solute transported (μmol), Δt is incubation time (sec), A is filter surface area in cm^2, and C_o is mean of starting-end drug concentration in the donor well (μM). Drug velocity is expressed as apparent permeability, P_{app}, with the unit 1 x 10^{-6}

cm/sec. Efflux Ratio (ER) = P_{app} (B-to-A)/P_{app} (A-to-B). An internal standard buspirone was added to all wells.

Protein Binding: Equilibrium dialysis was performed with the Rapid Equilibrium Dialysis (RED) equipment (Thermo Fisher Scientific, Schwerte, Germany) to determine binding to determine binding of analogs in both rat brain and plasma. A semi-permeable membrane separated a plasma or brain tissue (matrix) compartment from a matrix-free compartment with a potassium phosphate buffer. A sample of the specific matrix (500 µL plasma (sourced from Bioreclamation), brain homogenate (1:6 tissue to buffer ratio) from male, Sprague Dawley rats) was aliquoted into individual cluster tubes and to each tube was added 0.5 µL of 1 mM stock solution of compound in DMSO. After mixing by aspiration, 100 µL of the matrix/compound mixture was added to the dialysis plate in triplicate. The plate was sealed with an adhesive plate sealer and placed on an orbital shaker in an incubator, (150 rpm at 37°C) for 4 hrs. A quench solution of 50 nM carbutamide in 95:5 MeCN:MeOH was used and the samples were analyzed by LC-MS/MS. The fraction unbound (f_u) in plasma ($f_{u,plasma}$) or tissue ($f_{u,brain}$) = (calculated concentration in buffer/ calculated concentration in matrix). Imipramine was used as a positive control.

Rat PK: Male Sprague-Dawley rats, weighing 250–400 g, were obtained from Charles River Laboratories (Freiburg, Germany). Pharmacokinetic studies were conducted in groups of rats; each dosing group (IV, PO or IP) contained three animals. All groups were dosed with a solution formulation. Sequential blood samples were obtained from a tail vein of each animal for 8-24 hours after dosing. Plasma was separated by centrifugation and stored frozen until analysis. To determine the concentration of the compound in the brain, brain tissue was extracted after dosing at defined timepoints, and terminal plasma samples taken from the same animals. Compounds were selectively isolated from the plasma using either liquid/liquid extraction or protein

precipitation followed by reverse phase HPLC with MS/MS detection for quantitation. In more detail, animals were fasted overnight prior to dosing, with free access to water. Rats were allowed free access to food and water prior to and during dosing for assessing effect of dose, formulation and tissue pharmacokinetics. The intravenous dose in rat was administered as a slow bolus to the jugular vein under isoflurane anesthesia. Oral doses were administrated by gavage. Blood samples, collected into K2EDTA or K3EDTA anticoagulant for plasma concentration analysis, were obtained from each animal after dosing. Generally, 9 to 12 serial samples were obtained over a period of 24 to 48 hours post dosing in all animals. Plasma was separated by centrifugation (3000 or 4000 g x 10 minutes, ~4°C) and stored frozen (<-20°C) until analysis. Protein precipitation was generally done by adding 400 µL acetonitrile including an appropriate internal standard to 50 µL of plasma and mixed, followed by a 10 minute centrifugation at 2000 g at 4°C. 125 µL of the supernatant was removed and transferred to a 96-well plate, followed by LC-MS/MS analysis (AB Sciex API 4000, 5000 or 6500; AB Sciex Germany GmbH, Darmstadt, Germany) employing Waters Acquity HPLC systems (Waters GmbH, Eschborn Germany).

The total brain to plasma ratio (Kp)was calculated by C_{brain}/C_{plasma}. The free brain to plasma ratio (Kp,uu) was calculated according to $(C_{brain}/C_{plasma})*(f_{u,brain}/f_{u,plasma})$. Oral bioavailability was determined according to the dose-normalized ratio of PO over IV AUC

Animal Behavioral Studies. Materials and Methods. For *ex vivo* GlyT1 binding assay male, NMRI mice were obtained from Janvier (Le Genest-St-Isle, France) and were housed eight per cage (Macrolon, type III, unless specified otherwise). Animals had a body weight of approximately 26-28 g upon arrival. For L687,414-induced hyperlocomotion experiments, male C57Bl/6 mice were obtained from Janvier (Le Genest-Saint-Isle, France; five weeks old upon arrival) and were housed eight per cage (Macrolon, type III).

The animals were maintained under standard conditions (12 hours day/night cycle, light switched on at 0600 hours, room temperature 21±1°C, 55±15% humidity) with free access to food and tap water. Before being used for the experiments, the animals were allowed to recover from transportation for at least one week. All experiments were conducted during the light period of the light/dark cycle.

All experiments were conducted in facilities with full AAALAC accreditation in accordance with the recommendations and policies of the U.S. National Institutes of Health "Principles of laboratory animal care" (1996 edition), all applicable European and German laws and were approved by AbbVie's Animal Welfare Officer.

***Ex vivo* GlyT1 Binding Assay.** Animals were subjected to single housing one day before the experiment and transferred from the animal facility into the experimental room where they were housed in ventilated containers (Scantainer Type D, Scanbur Ltd., Denmark) until the next day. On the day of the experiment, the mice had a body weight of 28-34 g. Before the experiment, the animals were (pseudo-) randomly assigned to the different treatment groups consisting of five mice per group. The tested compounds or the vehicle was applied intraperitoneally (i.p.). For the determination of non-specific binding, five animals were treated with 100 mg/kg of SSR504734. One hour after drug application, the mice were anaesthetized with isoflurane, blood samples were taken by cardiac puncture. Immediately after blood sampling and still under anesthesia, animals were sacrificed by cervical dislocation. Forebrains were dissected, rapidly frozen in liquid nitrogen and stored at -80°C until investigated in the binding assay. For determination of the *ex vivo* GlyT1 binding, the dissected forebrains were homogenized in five volumes Tris-buffered saline (50 mM Tris-Cl, pH 7.4; 150 mM NaCl) with the UltraTurrax (9600 UPM, 15 seconds). 100 µL of the homogenate was mixed with 10 µL [^{3}H]N-methyl-SSR504734[13] to yield a final concentration of 5 nM (0.04 µCi/mL). Three aliquots of 20 µL were transferred to macrowell

vials, subjected to filtration with a scatron harvester 60 minutes after addition of the radioligand, and membrane bound radioactivity was determined by liquid scintillation counting. Forebrains from animals treated with 100 mg/kg SSR504734 were used for the determination of non-specific binding. Specific binding was determined by subtracting the mean binding of the vehicle- or SSR504734-treated animals from the total binding of each individual sample (triplicates for each animal). The apparent ED_{50} (mean ± S.E.M) was determined by non-linear curve fitting of the inhibition of specific radioligand binding (means of the individual animals) vs. the dose. From this value an ED_{50} for *in vivo* TO was estimated by dividing the apparent ED_{50} by 6.6. This estimation is based on the 6.6-fold dilution of tested compounds by the *ex vivo* processing of the brain tissue and the assumption of a new binding equilibrium in the binding assay. All nonlinear curve fittings were performed with SigmaPlot 8.0 using a three parametric logistic equation.

L687,414-Induced Hyperactivity Model. Non-habituated mice were injected i.p. with 50 mg/kg of L687,414[30] or its vehicle 15 min prior to the two-hour test. Compound **(7*S*,8*R*)-27a** (1, 3 and 10 mg/kg) or its vehicle was given i.p. prior to the test. Each treatment group consisted of eight animals. The data were acquired by Cage Rack Photobeam system (San Diego Instruments, San Diego, CA). The analyzed data were total movements (fine movements + ambulations) during the first 30 min of the test.

ASSOCIATED CONTENT

Supporting Information

The Supporting Information is available free of charge on the ACS Publications website at DOI:

Molecular formula strings (CSV), CEREP Profile of compounds **(7*S*,8*R*)-27a** and **(7*S*,8*R*)-51a**

AUTHOR INFORMATION

Corresponding Author

*E-mail: wilhelm.amberg@abbvie.com.

ORCID

Willi Amberg: 0000-0003-4019-8712

Present Addresses

§For Y.L.: Eli Lilly and Company; Lilly Corporate Center, Indianapolis Indiana 46285, United States.

Notes

The authors declare the following competing financial interest(s): The authors are current or former employees of AbbVie (or Abbott Laboratories prior to separation), and may own company stock.

⊥Y.L. and B.B. are former AbbVie employees.

ACKNOWLEDGMENTS

We thank the global Abbott/AbbVie GlyT1 project team, in particular R. Biesinger, H. Glesius, S. Heitz, M. Lauer, M. Lieberknecht, M. Metz-Garrecht, R. Scheuermann, M. Vierling for synthesis, C. Krack and the LU team for analytical support and. Design, study conduct, and financial support for this research were provided by AbbVie. AbbVie participated in the interpretation of data, review, and approval of the publication.

ABBREVIATIONS USED

BCS, biopharmaceutics classification system; BOC, *tert*-butyloxycarbonyl; BrettPhos, dicyclohexyl(2',4',6'-triisopropyl-3,6-dimethoxy-(1,1'-biphenyl)-2-yl)phosphine; CYP3A4, Cytochrome P450 3A4; CYP450, Cytochrome P450; DCM, dichloromethane; DMSO, dimethyl

sulfoxide; DMAP, *N*,*N*-dimethyl-4-aminopyridine; ER, efflux ratio; EtOH, ethanol; EtOAc, ethylacetate; GlyT1, glycine transporter 1; HBD, hydrogen bond donor, hERG, human ether-a-go-go related gene; HEPES, 4-(2-hydroxyethyl)-1-piperazineethanesulfonic acid; HTS, high throughput screening; i.p., intra peritoneal; *i*PrOH, *iso*-propanol; mClint, scaled metabolic intrinsic clearance; MDCK, Madin-Darby canine kidney cells; MDR1, multiple drug resistance 1; MeCN, acetonitrile; MeOH, methanol; MW, molecular weight; NMDA, N-methyl-D-aspartate; P-gp, permeability glycoprotein; p.o., per os; PSD-95, postsynaptic density protein 95; SAR, structure activity relationship; TO, target occupancy, TPSA, topological polar surface area; RT, room temperature; TFA, trifluoroacetic acid; XPhos, 2-Dicyclohexylphosphino-2′,4′,6′-triisopropylbiphenyl.

REFERENCES

(1) Javitt, D. C.; Zukin, S. R. Recent advances in the phencyclidine model of schizophrenia. *Am. J. Psychiatry* **1991**, *148*, 1301–1308.

(2) Luby, E. D.; Gottlieb, J. S.; Cohen, B. D.; Rosenbaum, G.; and Domino, E F. Model psychoses and schizophrenia. *Am. J. Psychiatry* **1962**, *119*, 61–67.

(3) Krystal, J. H.; Karper, L. P.; Seibyl, J. P.; Freeman, G. K.; Delaney, R.; Bremner, J. D.; Heninger, G. R.; Bowers, M B., Jr.; Charney, D. S. Subanesthetic effects of the noncompetitive NMDA antagonist, ketamine, in humans. Psychotomimetic, perceptual, cognitive, and neuroendocrine responses. *Arch. Gen. Psychiatry* **1994**, *51*, 199–214.

(4) Lahti, A. C.; Weiler, M. A.; Tamara Michaelidis, B. A.; Parwani, A.; Tamminga, C. A. Effects of ketamine in normal and schizophrenic volunteers. *Neuropsychopharmacology* **2001**, *25*, 455–467.

(5) Coyle, J. T. Glutamate and schizophrenia: beyond the dopamine hypothesis. *Cell. Mol. Neurobiol*. **2006**, *26*, 365–384.

(6) Carter, C. J. Schizophrenia susceptibility genes converge on interlinked pathways related to glutamatergic transmission and long-term potentiation, oxidative stress and oligodendrocyte viability. *Schizophr. Res*. **2006**, *86*, 1-14.

(7) Harrison, P. J.; Weinberger, D. R. Schizophrenia genes, gene expression, and neuropathology: on the matter of their convergence. *Mol. Psychiatry* **2005**, *10*, 40-68.

(8) Harrison P. J. Recent genetic findings in schizophrenia and their therapeutic relevance. *J. Psychopharmacol*. **2015**, *29*, 85-96.

(9) Anticevic A.; Cole M. W.; Repovs G.; Savic A.; Driesen N. R.; Yang G.; Cho Y. T.; Murray J. D.; Glahn D. C.; Wang X.-J.; Krystal J. H. Connectivity, pharmacology, and computation: toward a mechanistic understanding of neural system dysfunction in schizophrenia. *Front. Psychiatry.* **2013**, *4*, 169.

(10) Cubelos B.; Gimenez C.; Zafra F. Localization of the GLYT1 glycine transporter at glutamatergic synapses in the rat brain. *Cereb. Cortex* **2005**, *15*, 448-459.

(11) Cubelos, B; Gonzalez-Gonzalez, I. M.; Gimenez, C.; Zafra, F. The scaffolding protein PSD-95 interacts with the glycine transporter GLYT1 and impairs its internalization. *J. Neurochem*. **2005**, *95*, 1047-1058.

(12) Marek GJ, Behl B, Bespalov AY, Gross G, Lee Y, Schoemaker H. Glutamatergic (N-methyl-D-aspartate receptor) hypofrontality in schizophrenia: too little juice or a miswired brain? *Mol. Pharmacol*. **2010**, *77*, 317-326.

(13) Mezler, M.; Hornberger, W.; Mueller, R.; Amberg W., Martin S.; Braje, W.; Ochse, M.; Schoemaker, H.; Behl, B. Inhibitors of GlyT1 affect glycine transport via discrete binding sites. *Mol. Pharmacol*. **2008**, *74*, 1705-1715.

(14) Pinard, E.; Alanine, A.; Alberati, D.; Bender, M.; Borroni, E.; Bourdeaux, P.; Brom, V.; Burner, S.; Fischer, H.; Hainzl, D.; Halm, R.; Hauser, N.; Jolidon, S.; Lengyel, J.; Marty, H.-P.; Meyer, T.; Moreau, J.-L.; Mory, R.; Narquizian, R.; Nettekoven, M.; Norcross, R. D.; Puellmann, B.; Schmid, P.; Schmitt, S.; Stalder, H.; Wermuth, R.; Wettstein, J. G.; Zimmerli, D. Selective GlyT1 inhibitors: discovery of [4-(3-fluoro-5-trifluoromethylpyridin-2-yl)piperazin-1-yl][5-methanesulfonyl-2-((S)-2,2,2-trifluoro-1-methylethoxy)phenyl]methanone (RG1678), a promising novel medicine to treat schizophrenia. *J. Med. Chem.* **2010**, *53*, 4603-4614

(15) Gibson, S. G.; Jaap, D. R.; Thorn, S. N.; Gilfillan, R. Preparation of Aminomethylcarboxylic Acid Derivatives for Treatment of CNS Disorders. WO 2000007978, **2000**

(16) Lowe, J. A. 3rd; Drozda S. E.; Fisher K.; Strick C.; Lebel L.; Schmidt C.; Hiller D.; Zandi K. S. [^{3}H]-(R)-NPTS, a radioligand for the type 1 glycine transporter. *Bioorg. Med. Chem. Lett.* **2003**, *13*, 1291-1292

(17) Depoortere, R.; Dargazanli, G.; Estenne-Bouhtou, G.; Coste, A.; Lanneau, C.; Desvignes, C.; Poncelet, M.; Heaulme, M.; Santucci, V.; Decobert, M.; Cudennec, A.; Voltz, C.; Boulay, D.; Terranova, J. P.; Stemmelin, J.; Roger, P.; Marabout, B.; Sevrin, M.; Vige, X.; Biton, B.; Steinberg, R.; Francon, D.; Alonso, R.; Avenet, P.; Oury-Donat, F.; Perrault, G.; Griebel, G.; George, P.; Soubrie, P.; Scatton, B. Neurochemical, electrophysiological and pharmacological profiles of the selective inhibitor of the glycine transporter-1 SSR504734, a potential new type of antipsychotic. *Neuropsychopharmacology* **2005**, *30*, 1963-1985.

(18) Blackaby, W. P.; Lewis, R. T.; Thomson, J. L.; Jennings, A. S. R.; Goodacre, S. C.; Street, L. J.; MacLeod, A. M.; Pike, A.; Wood, S.; Thomas, S.; Brown, T. A.; Smith, A.; Pillai, G.; Almond, S.; Guscott, M. R.; Burns, H. D.; Eng, W.; Ryan, C.; Cook, J.; Hamill, T. G.

Identification of an orally bioavailable, potent, and selective inhibitor of GlyT1, ACS Med. Chem. Let. **2010**, *1*, 350-354.

(19) Lowe, J. A. 3rd; Hou X.; Schmidt C.; David T. F. 3rd; McHardy S.; Kalman M.; Deninno S.; Sanner M.; Ward K.; Lebel L.; Tunucci D.; Valentine J.; Bronk B. S.; Schaeffer E. The discovery of a structurally novel class of inhibitors of the type 1 glycine transporter. *J. Bioorg. Med. Chem. Lett.* **2009**, *19*, 2974-2976.

(20) Youngman, M. A.; Willard, N. M.; Dax, S. L.; McNally, J. J. The synthesis of novel cis-α-substituted-β-aminotetralins. *Synth. Commun.* **2003**, *33*, 2215-2227

(21) Meeuwissen, J; Kuil, M.; van der Burg, A.; Sandee, A.; Reek, J. Application of a supramolecular-ligand library for the automated search for catalysts for the asymmetric hydrogenation of industrially relevant substrates. *Chem. Eur. J.* **2009**, *15*, 10272-10279.

(22) Meeuwissen, J.; Detz, R. J.; Sandee, A. J.; de Bruin, B.; Reek, J. N. H. Rhodium-P,O-bidentate coordinated ureaphosphine ligands for asymmetric hydrogenation reactions. *Dalton Trans.* **2010**, *39*, 1929-1931.

(23) Dupau, P.; Bruneau, C.; Dixneuf, P. Enantioselective hydrogenation of the tetrasubstituted C=C bond of enamides catalyzed by a ruthenium catalyst generated in situ. *Adv. Synth. Catal*. **2001**, *343*, 331-334

(24) Dijkstra, D.; Mulder, T. B. A.; Rollema, H.; Tepper, P. G.; Van der Weide, J.; Horn, A. S. Synthesis and pharmacology of *trans*-4-*n*-propyl-3,4,4a,10b-tetrahydro-2*H*,5*H*-1-benzopyrano[4,3-b]1,4-oxazin-7- and -9-ols. The significance of nitrogen pk_a values for central dopamine receptor activation. *J. Med. Chem.* **1988**, *31*, 2178-2182.

(25) Thomson, J. L.; Blackaby, W. P.; Jennings, A. S. R.; Goodacre, S. C.; Pike, A.; Thomas, S.; Brown, T. A.; Smith, A.; Pillai, G.; Street, L. J.; Lewis, R. T. Optimisation of a series of

potent, selective and orally bioavailable GlyT1 inhibitors. *Bioorg. Med. Chem. Lett.* **2009**, *19*, 2235-2239.

(26) Doan, K. M. M.; Humphreys, J. E.; Webster, L. O.; Wring, S. A.; Shampine, L. J.; Serabjit-Singh, C. J.; Adkison, K. K.; Polli, J. W. Passive permeability and P-glycoprotein-mediated efflux differentiate central nervous system (CNS) and non-CNS marketed drugs. *J. Pharmacol. Exp. Ther.* **2002**, *303*, 1029 –1037.

(27) Wager, T. T.; Chandrasekaran, R. Y.; Hou, X.; Troutman, M. D.; Verhoest, P. R.; Villalobos, A.; Will, Y. Defining desirable central nervous system drug space through the alignment of molecular properties, *in vitro* ADME, and safety attributes. *ACS Chem. Neurosci.* **2010**, *1*, 420–434.

(28) Ghose, A. K.; Herbertz, T.; Hudkins, R. L.; Dorsey, B. D.; Mallamo, J. P. Knowledge-based, central nervous system (CNS) lead selection and lead optimization for CNS drug discovery. *ACS Chem. Neurosci.* **2012**, *3*, 50-68.

(29) Alberati D.; Moreau J.-L.; Mory R.; Pinard E.; Wettstein J. G. Pharmacological evaluation of a novel assay for detecting glycine transporter 1 inhibitors and their antipsychotic potential. *Pharmacol. Biochem. Behav.* **2010**, *97*, 185-191.

(30) Pinard, E.; Burner, S.; Cueni, P.; Montavon, F.; Zimmerli, D. A short and efficient synthesis of the NMDA glycine site antagonist: (3*R*,4*R*)-3-amino-1-hydroxy-4-methyl pyrrolidin-2-one (L-687,414). *Tetrahedron Letters* **2008**, *49*, 6079-6080.

(31) Hitchcock, S. A. Structural modifications that alter the P-glycoprotein efflux properties of compounds. *J. Med. Chem.* **2012**, *55*, 4877-4895.

(32) Didziapetris, R.; Japertas, P.; Avdeef, A.; Petrauskas, A. Classification analysis of P-glycoprotein substrate specificity. *J. Drug Targeting* **2003**, *11*, 391−406.

(33) Wager, T. T.; Hou, X.; Verhoest, P. R.; Villalobos, A. Moving beyond rules: The development of a central nervous system multi-parameter optimization (CNS MPO) approach to enable alignment of drug-like properties. *ACS Chem. Neurosci.* **2010**, *1*, 435-449.

(34) Rankovic, Z. CNS drug design: balancing physicochemical properties for optimal brain exposure. *J. Med. Chem.* **2015**, *58*, 2584−2608.

(35) Johnson, J. W.; Ascher, P. Equilibrium and kinetic study of glycine action on the N-methyl-D-aspartate receptor in cultured mouse brain neurons. *J. Physiol.* **1992**, *455*, 339-365.

(36) Kleckner, N. W.; Dingledine, R. Requirement for glycine in activation of NMDA-receptors expressed in xenopus oocytes. *Science* **1988**, *241*, 835-837.

(37). Schmieden V.; Betz H. Pharmacology of the inhibitory glycine receptor: agonist and antagonist actions of amino acids and piperidine carboxylic acid compounds. *Mol. Pharmacol*. **1995**, *48*, 919-927.

(38). Langosch, D.; Laube, B.; Rundstrom, N.; Schmieden, V.; Bormann, J.; Betz, H. Decreased agonist affinity and chloride conductance of mutant glycine receptors associated with human hereditary hyperekplexia. *EMBO J*. **1994**, *13*, 4223-4228.

(39) Chen, R.-Q.; Wang, S.-H.; Yao, W.; Wang, J.-J.; Ji, F.; Yan, J.-Z.; Ren, S.-Q.; Chen, Z.; Liu, S.-Y.; Lu, W. Role of glycine receptors in glycine-induced LTD in hippocampal CA1 pyramidal neurons. *Neuropsychopharmacology* **2011**, *36*, 1948-1958.

(40). Alberati, D.; Moreau, J.-L.; Lengyel, J.; Hauser, N.; Mory, R.; Borroni, E.; Pinard, E.; Knoflach, F.; Schlotterbeck, G.; Hainzl, D. Wettstein, J. G. Glycine reuptake inhibitor RG1678: a pharmacologic characterization of an investigational agent for the treatment of schizophrenia. *Neuropharmacol.* **2012**, *62*, 1152-1161.

(41). Nong Y.; Huang Y.-Q.; Ju W.; Kalia L. V.; Ahmadian G.; Wang Y. T.; Salter M. W. Glycine binding primes NMDA receptor internalization. *Nature* **2003**, *422*, 302-307.

(42) Seibert, R.; Abbasi, F.; Hantash, F. M.; Caulfield, M. P.; Reaven, G.; Kim, S. H. Relationship between insulin resistance and amino acids in women and men. *Physiol. Rep.* **2015**, *3*, e12392

(43) Winter, M.; Funk, J.; Korner, A.; Alberati, D.; Christen, F.; Schmitt, G.; Altmann, B.; Pospischil, A.; Singer, T. Effects of GlyT1 inhibition on erythropoiesis and iron homeostasis in rats. *Exp. Hematol.* **2016**, *44*, 964-974.

(44) Amberg, W.; Ochse, M.; Lange, U.; Kling, A.; Behl, B.; Hornberger, W.; Mezler, M.; Hutchins, C. Aminotetraline Derivatives as GlyT1 Inhibitors and Their Preparation, Pharmaceutical Compositions Containing Them, and Their Use in Therapy. WO 2010092180, **2010**.

(45) Amberg, W.; Pohlki, F.; Lange, U.; Wang, Y.; Zhao, H.; Li, H.-Q.; Brewer, J.; Vasudevan, A.; Lao, Y.; Hutchins, C. W. Aminotetraline and Aminoindane Derivatives, Pharmaceutical Compositions Containing Them, and Their Use in Therapy. WO 2015055771, **2015**.

(46) Amberg, W.; Pohlki, F.; Lange, U.; Wang, Y.; Zhao, H.; Li, H.-Q.; Brewer, J.; Vasudevan, A.; Lao, Y.; Hutchins, C. W. Aminochromane, Aminothiochromane and Amino-1,2,3,4-tetrahydroquinoline Derivatives, Pharmaceutical Compositions Containing Them, and Their Use in Therapy. WO 2015055770, **2015**.

(47) Munson, P. J.; Rodbard, D. Ligand: a versatile computerized approach for characterization of ligand-binding systems. *Anal. Biochem.* **1980**, *107*, 220–239.

(48) Cheng, Y.; Prusoff, W. H. Relationship between the inhibition constant (K_i) and the concentration of inhibitor which causes 50 per cent inhibition (I_{50}) of an enzymatic reaction. *Biochem. Pharmacol.* **1973**, *22*, 3099–3108.

(49) Liman, E. R.; Tytgat, J.; and Hess P. Subunit stoichiometry of a mammalian K^+ channel determined by construction of multimeric cDNAs. *Neuron* **1992**, *9*, 861–871.

(50) Frost, J. M.; DeGoey, D. A.; Shi, L.; Gum, R. J.; Fricano, M. M.; Lundgaard, G. L.; El-Kouhen, O. F.; Hsieh, G. C.; Neelands, T.; Matulenko, M. A.; Daanen, J. F.; Pai, M.; Ghoreishi-Haack, N.; Zhan, C.; Zhang; X.-F.; Kort, M. E. Substituted indazoles as Nav1.7 blockers for the treatment of pain. *J. Med. Chem.* **2016**, *59*, 3373-3391

(51) Gartzke, D.; Delzer, J.; Laplanche, L.; Uchida, Y.; Hosh,i Y.; Tachikawa, M.; Terasaki, T.; Sydor,J.; Fricker, G. Genomic knockout of endogenous canine P-clycoprotein in wild-type, human P-glycoprotein and human BCRP transfected MDCKII cell lines by zinc finger. *Pharm. Res.* **2015**, *32*, 2060-2071

Figure for Table of Content

pp

Publication Date (Web):

DOI:

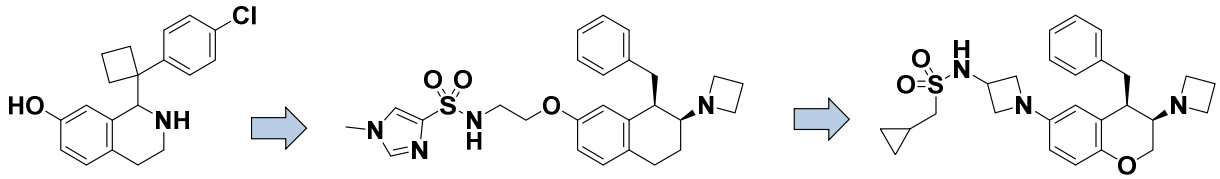

7

K_i hGlyT1 = 124 nM
Low selectivity vs
several receptors

(7*S*,8*R*)-27a

K_i hGlyT1 = 2.6 nM
Efflux ratio = 12

High selectivity

51b

K_i hGlyT1 = 18 nM
Efflux ratio = 1